

Efficient Estimation of Pairwise Effective Resistance

RENCHI YANG*, Hong Kong Baptist University, Hong Kong SAR

JING TANG†, The Hong Kong University of Science and Technology (Guangzhou), China and The Hong Kong University of Science and Technology, Hong Kong SAR

Given an undirected graph G , the effective resistance $r(s, t)$ measures the dissimilarity of node pair s, t in G , which finds numerous applications in real-world scenarios, such as recommender systems, combinatorial optimization, molecular chemistry and electric power networks. Existing techniques towards pairwise effective resistance estimation either trade approximation guarantees for practical efficiency, or vice versa. In particular, the state-of-the-art solution is based on a multitude of Monte Carlo random walks, rendering it rather inefficient in practice especially on large graphs.

Motivated by this, this paper first presents an improved Monte Carlo approach, AMC, which reduces both the length and amount of random walks required without degrading the theoretical accuracy guarantee, through careful theoretical analysis and an adaptive sampling scheme. Further, we develop a greedy approach, GEER, which combines AMC with sparse matrix-vector multiplications in an optimized and non-trivial way. GEER offers significantly improved practical efficiency over AMC without compromising its asymptotic performance and accuracy guarantees. Extensive experiments on multiple benchmark datasets reveal that GEER is orders of magnitude faster than the state of the art in terms of computational time when achieving the same accuracy.

CCS Concepts: • **Mathematics of computing** → **Graph algorithms**; • **Theory of computation** → **Random walks and Markov chains**.

Additional Key Words and Phrases: Effective Resistance, Random Walk, Matrix Multiplication

ACM Reference Format:

Renchi Yang and Jing Tang. 2023. Efficient Estimation of Pairwise Effective Resistance. *Proc. ACM Manag. Data* 1, 1, Article 16 (May 2023), 28 pages. <https://doi.org/10.1145/3588696>

1 INTRODUCTION

Given an undirected graph G and two nodes $s, t \in G$, the *effective resistance* (ER) [65] $r(s, t)$ is proportional to the expected number of steps taken by a random walk starting at s visits node t and then goes back to s (i.e., the *commute time* [13] between s and t). Intuitively, a small $r(s, t)$ suggests a high similarity between nodes s and t . Due to the clear physical meaning and unique properties, ER finds a variety of applications in practical problems. For instance, in the study of electric circuits [47], resistive electrical networks are viewed as graphs where each edge corresponds to a resistor. The definition of ER $r(s, t)$ is basically the voltage developed between nodes s and t when a unit current is injected at one and extracted at the other [65]. Intuitively, this physical interpretation benefits analyzing cascading failures [26, 59] and power network stability [22, 60, 61]

*Work was done when the first author was a Research Fellow at NUS, Singapore.

†Corresponding author: Jing Tang.

Authors' addresses: [Renchi Yang](mailto:renchi@hkbu.edu.hk), Department of Computer Science, Hong Kong Baptist University, Hong Kong SAR, renchi@hkbu.edu.hk; [Jing Tang](mailto:jingtang@ust.hk), The Hong Kong University of Science and Technology (Guangzhou), China and The Hong Kong University of Science and Technology, Hong Kong SAR, jingtang@ust.hk.

Permission to make digital or hard copies of all or part of this work for personal or classroom use is granted without fee provided that copies are not made or distributed for profit or commercial advantage and that copies bear this notice and the full citation on the first page. Copyrights for components of this work owned by others than the author(s) must be honored. Abstracting with credit is permitted. To copy otherwise, or republish, to post on servers or to redistribute to lists, requires prior specific permission and/or a fee. Request permissions from permissions@acm.org.

© 2023 Copyright held by the owner/author(s). Publication rights licensed to ACM.

2836-6573/2023/5-ART16 \$15.00

<https://doi.org/10.1145/3588696>

in electric power networks. Moreover, Spielman and Srivastava [62] theoretically proved that sampling edges in a graph G according to their ER values yields a high-quality sparsified graph with a rigorous accuracy guarantee. Such graph sparsifiers are used as building blocks to accelerate cut approximation [10], max-flow algorithms [15, 33], and solving linear systems [63]. In recent years, ER is further applied to many data mining problems such as graph clustering [2, 51, 79], recommender systems [24, 36], and image segmentation [9, 50]. Additionally, the data management community adopts ER in developing efficient graph systems [52, 81] and applications [57, 64, 80].

As explained in Section 2.2, the exact computation of ER incurs vast computational costs for large graphs; and thus, the majority of existing work (e.g., [7, 12, 18, 29, 31, 49]) focuses on computing approximate ER. In the meanwhile, it is prohibitively expensive to materialize the ER values of all possible node pairs in a large graph due to the colossal space, i.e., $O(n^2)$, where n is the number of nodes in G . To this end, recent work [18, 49] on ER computation answers the ϵ -approximate pairwise effective resistance (denoted hereinafter as ϵ -approximate PER) query for each specified node pair individually. More precisely, given an additive error ϵ and a node pair (s, t) in the input graph G , an ϵ -approximate PER query returns an approximate ER $r'(s, t)$ with at most ϵ additive error in it. Even under the approximation definition, ϵ -approximate PER computation remains tenaciously challenging to address owing to its complicated definitions by either the pseudo inverse of matrix or random walks.

Andoni et al. [5] introduced an algorithm for answering ϵ -approximate PER queries on regular expander graphs using a time complexity of $O\left(\frac{1}{\epsilon^2} \text{polylog}\left(\frac{1}{\epsilon}\right)\right)$. Spielman and Srivastava [62] described a random projection-based algorithm, which allows for the ϵ -approximate PER query of any node pair in G to be answered in $O(\log n)$ time. However, their algorithm requires $\tilde{O}(m/\epsilon^2)$ time (m is the number of edges in G) for constructing a $(24 \log n/\epsilon^2) \times n$ matrix in the preprocessing step, which is prohibitive for large graphs. Very recently, a suite of randomized techniques without any preprocessing are proposed in [49] for addressing ϵ -approximate PER computation on general graphs with provable performance guarantees. Among them, MC simulates numerous random walks from source node s to estimate $r(s, t)$ according to its *commute time*-based interpretation mentioned previously. Nevertheless, this way is highly inefficient in practice as its random walks explore the whole graph, resulting in a large time complexity of $O\left(\frac{m \cdot d(s)}{\epsilon^2}\right)$, where $d(s)$ represents the degree of node s . To circumvent this problem, Peng et al. [49] subsequently propose a new ϵ -approximate PER solution TP based on another random walk-based interpretation of ER. This interpretation enables the derivation of a maximum length for random walks, and thus TP only explores a small portion of G . In turn, TP runs in $O\left(\frac{1}{\epsilon^2} \log^4\left(\frac{1}{\epsilon}\right)\right)$ expected time regardless of the size of G . TPC subsequently ameliorates TP by leveraging the idea of stitching short random walks to longer ones, yielding a time cost of $O\left(\frac{1}{\epsilon^2} \log^3\left(\frac{1}{\epsilon}\right)\right)$ on expander graphs. Although these algorithms achieve significant improvements upon previous solutions in terms of asymptotic performance, they still entail an exorbitant amount of time in practice, even on small graphs. This is caused by the sheer number of long random walks required by them, leaving much room for improvement regarding computational costs.

Contributions. This paper first presents AMC, an adaptive Monte Carlo approach that overcomes the deficiencies of TP and TPC, while retaining the accuracy assurance. More precisely, AMC derives a refined maximum random walk length through a rigorous theoretical analysis. Moreover, instead of simulating a fixed number of random walks, AMC conducts random walks in an adaptive fashion by leveraging the empirical Bernstein inequality to facilitate early termination. In particular, our refined maximum random walk length ℓ is often less than half of its counterpart in prior work

Table 1. Algorithms for ϵ -approximate PER Queries

Algorithm	Time Complexity
TP [49]	$O\left(\frac{1}{\epsilon^2} \log^4\left(\frac{1}{\epsilon}\right)\right)$
TPC [49]	$O\left(\frac{1}{\epsilon^2} \log^3\left(\frac{1}{\epsilon}\right)\right)$ on expander graphs
MC [49]	$O\left(\frac{m \cdot d(s)}{\epsilon^2}\right)$
our AMC and GEER	$O\left(\frac{1}{\epsilon^2 d^2} \log^3\left(\frac{1}{\epsilon d}\right)\right)$

[49] and the well-thought-out adaptive scheme in AMC leads to over $20\times$ reduction in random walk samples, compared to the state-of-the-art Monte Carlo approach TP. Unfortunately, despite the aforementioned optimizations in AMC enable a significant reduction in computational cost, its practical efficiency is still less than satisfactory, as revealed in our empirical studies. For this purpose, we develop our main proposal GEER for improved practical efficiency. Under the hood, the core of GEER is to integrate sparse matrix-vector multiplications into AMC in an optimized and non-trivial way, thereby overcoming the drawbacks of both and achieving significantly enhanced speedup compared to AMC without degrading the theoretical guarantees. Table 1 compares the time complexities of our proposed solutions against three approximate algorithms to answer ϵ -approximate PER queries with a high probability. We can see that both AMC and GEER achieve the best asymptotic performance, i.e., $O\left(\frac{1}{\epsilon^2 d^2} \log^3\left(\frac{1}{\epsilon d}\right)\right)$, which theoretically improves the state of the art by a large factor of $d^2 \log\left(\frac{1}{\epsilon d}\right)$, where d equals $\min\{d(s), d(t)\}$ and $d(s)$ (resp. $d(t)$) represents the degree of node s (resp. t). In practice, on the the widely studied Friendster dataset, GEER is up to $38.2\times$ faster than AMC and achieves more than three orders of magnitude enhancements over the state of the art in query performance. Briefly, our key contributions in this paper can be summarized as follows:

- We propose AMC, an adaptive Monte Carlo algorithm runs in $O\left(\frac{1}{\epsilon^2 d^2} \log^3\left(\frac{1}{\epsilon d}\right)\right)$ expected time and returns an ϵ -approximate ER value with a high probability.
- We further develop GEER, which offers significantly improved empirical efficiency over AMC without compromising the asymptotic guarantees.
- Extensive experiments using real datasets demonstrate that on a single commodity server GEER consistently outperforms the state-of-the-art solution often by orders of magnitude speedup.

The remainder of the paper is organized as follows. In Section 2, we provide notations and formally define the problem. We present our first-cut solution AMC with theoretical analysis in Section 3, and further propose an improved solution GEER in Section 4. Our solutions and existing methods are evaluated in Section 5. Related work is reviewed in Section 6. Finally, Section 7 concludes the paper. All proofs of theorems and lemmas appear in Appendix A.

2 PRELIMINARIES

This section first defines common notations, and then provides the formal problem definition and revisits main competitors.

2.1 Notations

We denote vectors \vec{x} and matrices \mathbf{X} in bold lower and upper cases, respectively, and use $\vec{x}(i)$ to represent the i -th element of vector \vec{x} . In addition, \vec{e}_i is used to denote a one-hot vector, which has value 1 at entry i and 0 everywhere else. Row-wise (i.e., $\mathbf{X}(i)$), column-wise (i.e., $\mathbf{X}(, j)$), and element-wise (i.e., $\mathbf{X}(i, j)$) matrix indexing represent the i -th row vector, j -th column vector, and

Table 2. Frequently used notations

Notation	Description
$G = (V, E)$	\triangleq An undirected and unweighted graph with node set V and edge set E .
n, m	\triangleq The numbers of nodes and edges in graph G , respectively.
\mathbf{P}	\triangleq The transition matrix of G .
$d(v)$	\triangleq The degree of node v .
$r(s, t)$	\triangleq The effective resistance between nodes s, t .
$r'(s, t)$	\triangleq The approximate version of $r(s, t)$.
$r_\ell(s, t)$	\triangleq The ℓ -truncated version of $r(s, t)$ (see Eq. (4)).
λ_i	\triangleq The i -th largest eigenvalue of \mathbf{P} .
$p_i(u, v)$	\triangleq The probability of a length- i random walk starting from node u ending at node v .
ϵ, δ	\triangleq The absolute error threshold and the failure probability, respectively.
τ	\triangleq The number of batches of random walks in AMC.
ℓ	\triangleq The maximum random walk length (see Eq. (6)).
ℓ_f	\triangleq The maximum random walk length in AMC.
ℓ_b	\triangleq The number of iterations in SMM.
$\min(\vec{\mathbf{x}})$	\triangleq The smallest value in vector $\vec{\mathbf{x}}$.
$\max_k(\vec{\mathbf{x}})$	\triangleq The k -th largest value in vector $\vec{\mathbf{x}}$.

the scalar at i -th row and j -th column of \mathbf{X} , respectively. We denote by $\min(\vec{\mathbf{x}})$ and $\max_k(\vec{\mathbf{x}})$ the smallest value and the k -th largest value in vector $\vec{\mathbf{x}}$, respectively.

We are given an undirected and unweighted graph $G = (V, E)$ with $|V| = n$ nodes and $|E| = m$ edges. For each node $v \in V$, we denote by $d(v)$ its degree, i.e., the number of neighbors connecting to v . Let \mathbf{A} and \mathbf{D} be the *adjacency matrix* and *diagonal degree matrix* of G , respectively; i.e., $\mathbf{A}(u, v) = 1$ iff $(u, v) \in E$ and each diagonal entry $\mathbf{D}(v, v) = d(v) \forall v \in V$. The random walk matrix (a.k.a. transition matrix) of G is then defined as $\mathbf{P} = \mathbf{D}^{-1}\mathbf{A}$; i.e., $\mathbf{P}(u, v) = \frac{1}{d(v)}$ if $(u, v) \in E$. Accordingly, $p_i(u, v) = \mathbf{P}^i(u, v)$ signifies the probability of a length- i simple random walk starting from node u ending at node v . For simplicity, we henceforth refer to a simple random walk as a random walk, which at each visited node v , moves to a neighbor of v with probability $\frac{1}{d(v)}$ [40]. Throughout this paper, we assume that G is connected and non-bipartite, inducing that \mathbf{P} is ergodic; in other words, $\lim_{i \rightarrow \infty} \vec{\mathbf{e}}_s \mathbf{P}^i = \vec{\pi} \forall s \in V$, where $\vec{\pi}(v) = \frac{d(v)}{2m} \forall v \in V$ [45]. Let $\lambda_1, \lambda_2, \dots, \lambda_n$ be the eigenvalues of \mathbf{P} , sorted by algebraic value in descending order, i.e., $1 = \lambda_1 \geq \lambda_2 \geq \dots \geq \lambda_n \geq -1$. Let $\mathbb{1}_{s \neq t}$ be an indicator function, which is equal to 1 if $s \neq t$ and otherwise 0. Table 2 lists the frequently used notations throughout this paper.

2.2 Problem Definition

Definition 2.1 (Effective Resistance (ER)). Given graph G and two nodes $s, t \in G$, the effective resistance between s and t is defined as

$$r(s, t) = (\vec{\mathbf{e}}_s - \vec{\mathbf{e}}_t) \cdot \mathbf{L}^\dagger \cdot (\vec{\mathbf{e}}_s - \vec{\mathbf{e}}_t)^\top, \quad (1)$$

where \mathbf{L}^\dagger denotes the Moore-Penrose pseudo-inverse of $\mathbf{D} - \mathbf{A}$.

Definition 2.1 presents the formal definition of effective resistance (ER). In particular, the ER $r(s, t)$ of node pair (s, t) is 0 when $s = t$, which indicates that any node $s \in G$ has zero dissimilarity to itself. In the literature [46, 65], ER is closely related to *commute time*. More precisely, $r(s, t) = \frac{c(s, t)}{2m}$, where $c(s, t)$ stands for the commute time between nodes s and t , i.e., the expected length of a random walk from s to visit t and return back to s .

The exact computation of $r(s, t)$ based on Definition 2.1 is immensely expensive as it requires inverting the Laplacian matrix of G with a time complexity of $O(n^{2.3727})$ [19, 53]. Prior work [49]

pertaining to ER computation proposes to compute ϵ -approximate ER. In particular, we say $r'(s, t)$ an ϵ -approximate ER of $r(s, t)$ if it satisfies

$$|r(s, t) - r'(s, t)| \leq \epsilon. \quad (2)$$

In this paper, we focus on addressing the ϵ -approximate PER query, as defined in Definition 2.2.

Definition 2.2 (ϵ -approximate PER Query). Given an undirected graph G and an arbitrarily small additive error ϵ , the ϵ -approximate PER query returns an ϵ -approximate ER value $r'(s, t)$ for any specified node pair (s, t) .

2.3 Main Competitors

In the rest of the section, we briefly overview four recent solutions proposed in [49] for answering ϵ -approximate PER queries and then discuss their limitations.

2.3.1 The MC and MC2 Algorithms. Using the connection between ER and commute time, MC [49] computes approximate $r(s, t)$ by first estimating the commute time $c(s, t)$ of node pair (s, t) . Recall that $c(s, t)$ is defined as the expected length of a random walk starting from s to visit t and return back to s . MC conducts Monte Carlo simulations using η random walks. That is, it counts the number η_r of random walks traverses from s to t and back, and then computes an approximate ER $r'(s, t)$ as $\frac{\eta}{d(s) \cdot \eta_r}$. Under the assumption $r(s, t) \leq \gamma$, Peng et al. [49] showed when $\eta = \frac{3\gamma d(s) \cdot \log(1/\delta)}{\epsilon^2}$, $r'(s, t)$ is an ϵ -approximate ER with a probability at least $1 - \delta$. The running time of MC is $O\left(\frac{md(s)\gamma^2}{\epsilon^2}\right)$. Notice that $c(s, t) < n^3$, and thus $r(s, t) < \frac{n^3}{2m}$ (Corollary 6.7 in [45]). Therefore, in the worst case, the time complexity of MC can be up to $O\left(\frac{n^6 d(s)}{m\epsilon^2}\right)$.

Regarding the special case where the query node pair (s, t) is connected by an edge in G (i.e., $(s, t) \in E$), Peng et al. [49] presented MC2 to support more efficient ϵ -approximate PER queries. Specifically, MC2 relies on the special definition of $r(s, t)$ when $(s, t) \in E$; that is, $r(s, t)$ is the probability that a random walk started at s visits t for the first time using the edge (s, t) . Accordingly, MC2 estimates $r(s, t)$ by performing such Monte Carlo random walks. By [49], with the assumption $r(s, t) > \gamma$, MC2 returns ϵ -approximate ER $r'(s, t)$ with a probability at least $1 - \delta$ after $\frac{3\log(1/\delta)}{\epsilon^2\gamma}$ random walks are conducted. Using the fact that $\frac{1}{2m} \leq r(s, t) \leq 1$, $\forall (s, t) \in E$ (Lemma 6.5 in [45]), the total number of random walks required in MC2 is bounded by $\frac{6m\log(1/\delta)}{\epsilon^2}$.

2.3.2 The TP and TPC Algorithms. In Lemma 4.3 of [49], the authors proved $L^\dagger = \sum_{i=0}^{\infty} P^i D^{-1}$, and further converted ER $r(s, t)$ in Eq. (1) into an equivalent form as follows:

$$r(s, t) = \sum_{i=0}^{\infty} \left(\frac{p_i(s, s)}{d(s)} + \frac{p_i(t, t)}{d(t)} - \frac{p_i(s, t)}{d(t)} - \frac{p_i(t, s)}{d(s)} \right), \quad (3)$$

where $p_i(s, t)$ denotes the probability of a length- i random walk from s visiting t . Notice that $r(s, t)$ in Eq. (3) involves summing up an infinite series of random walk probabilities, which is infeasible in practice. To this end, Peng et al. [49] propose to approximate its truncated version $r_\ell(s, t)$ as defined in Eq. (4):

$$r_\ell(s, t) = \sum_{i=0}^{\ell} \left(\frac{p_i(s, s)}{d(s)} + \frac{p_i(t, t)}{d(t)} - \frac{p_i(s, t)}{d(t)} - \frac{p_i(t, s)}{d(s)} \right), \quad (4)$$

where ℓ satisfies

$$\ell = \left\lceil \ln\left(\frac{4}{\epsilon - \epsilon\lambda}\right) / \ln\left(\frac{1}{\lambda}\right) - 1 \right\rceil, \text{ and } \lambda = \max\{|\lambda_2|, |\lambda_n|\}. \quad (5)$$

By setting the maximum random walk length ℓ as in Eq. (5), we can ensure $|r(s, t) - r_\ell(s, t)| \leq \frac{\epsilon}{2}$.

On the basis of the new problem formulation, two randomized algorithms TP and TPC are proposed in [49], which are the state-of-the-art solutions for ϵ -approximate PER computation. Both of them are to find an approximation $r'(s, t)$ of $r_\ell(s, t)$, such that $|r_\ell(s, t) - r'(s, t)| \leq \frac{\epsilon}{2}$.

LEMMA 2.3 (Hoeffding's Inequality [30]). *Let Z_1, Z_2, \dots, Z_{n_z} be independent random variables with Z_i ($\forall 1 \leq i \leq n_z$) is strictly bounded by the interval $[a_j, b_j]$. We define the empirical mean of these variables by $Z = \frac{1}{n_z} \sum_{i=1}^{n_z} Z_i$. Then, we have*

$$\mathbb{P}[|Z - \mathbb{E}[Z]| \geq \epsilon] \leq 2 \exp\left(-\frac{2n_z^2 \epsilon^2}{\sum_{j=1}^{n_z} (b_j - a_j)^2}\right).$$

Basically, TP is inspired by the simple and straightforward idea of Monte Carlo approach. More specifically, it simulates random walks of length ranging from 1 to ℓ from nodes s or t , records the fraction of them ending at s or t , and finally aggregates all these values into $r'(s, t)$ by the formula in Eq. (4). Applying the Chernoff-Hoeffding inequality derives that a total of $\frac{40\ell^2 \ln(8\ell/\delta)}{\epsilon^2}$ random walks are required for each length $i \in [1, \ell]$ so as to attain the desired ϵ -approximation with a success probability at least $1 - \delta$. TP suffers from severe efficiency issues, even on small graphs, by reason of a huge number of random walk samples as well as the large random walk length ℓ (up to thousands when ϵ is small).

Unlike TP, which directly estimates $p_i(s, t)$ via length- i ($i \in [1, \ell]$) random walks, TPC achieves a better theoretical bound by regarding $p_i(s, t)$ as a collision probability of two random walks of length $i/2$, $\forall 1 \leq i \leq \ell$. TPC samples $40000 \times \left(\ell \sqrt{\ell \beta_i} / \epsilon + \ell^3 \beta_i^{3/2} / \epsilon^2\right)$ length- $i/2$ random walks from nodes s and t , respectively, where the key parameter β_i is required to satisfy the inequality $\beta_i \geq \max\left\{\sum_{v \in V} \frac{p_i(s, v)^2}{d(v)}, \sum_{v \in V} \frac{p_i(t, v)^2}{d(v)}\right\}$. This requirement makes TPC impractical since the parameter β_i is unknown and hard to estimate.

3 AN ADAPTIVE MONTE CARLO APPROACH

In this section, we present AMC, an *Adaptive Monte Carlo* algorithm, for ϵ -approximate PER processing. AMC is similar in spirit to TP in that it first derives a maximum random walk length ℓ and then samples truncated random walks to estimate $r(s, t)$. The crucial differences are two-fold. First, contrary to the generic ℓ in Eq. (5), we offer a refined and individual ℓ for each node pair $(s, t) \in V \times V$ through a rigorous theoretical analysis (Section 3.1). Second, with the help of empirical Bernstein inequality, we tweak the random walk sampling such that it runs in an adaptive fashion; that is to say, it can terminate early under certain conditions without sacrificing any accuracy (Section 3.2). In addition, a theoretical analysis regarding correctness and complexity is given in Section 3.3 to indicate its superiority over TP.

3.1 Refining Maximum Length ℓ

The *mixing time* [20] ξ_s with respect to a source node s is the number of steps taken by a random walk from s to converge to the stationary distribution $\bar{\pi}$ of the graph. Note that mixing times vary from node to node and are directly associated with their neighborhoods [20]. In particular, when we set $\ell = \max\{\xi_s, \xi_t\}$, by Eq. (4) we can obtain $r(s, t) = r_\ell(s, t)$. Intuitively, given the same ℓ , $r_\ell(s, t)$ of a node pair (s, t) with low mixing times is more likely to be close to $r(s, t)$ compared to the case where the node pairs have high mixing times. To put it from another way, the maximum random walk length ℓ required to ensure $|r(s, t) - r_\ell(s, t)| \leq \frac{\epsilon}{2}$ is small if the mixing times pertaining to nodes s, t are low. However, in TP and TPC, they provide a large and generic ℓ (i.e., Eq. (5)) for all node pairs, regardless of the structural property surrounding each node, adversely impacting their

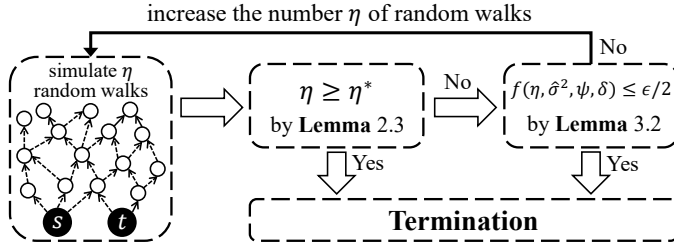


Fig. 1. Overview of AMC

performance. To remedy this problem, we offer an improved and personalized ℓ for different node pairs in Theorem 3.1 by capitalizing on the properties of eigenvalues and eigenvectors of \mathbf{P} .

THEOREM 3.1. *Given a graph G , $|r(s, t) - r_\ell(s, t)| \leq \frac{\epsilon}{2}$ holds for any two nodes s, t in G when ℓ satisfies*

$$\ell = \left\lceil \log \left(\frac{\frac{2}{d(s)} + \frac{2}{d(t)}}{\epsilon(1-\lambda)} \right) \middle/ \log \left(\frac{1}{\lambda} \right) - 1 \right\rceil, \text{ where } \lambda = \max\{|\lambda_2|, |\lambda_n|\}. \quad (6)$$

Compared to Peng et al.'s ℓ in Eq. (5), our refined ℓ in Eq. (6) incorporates node degrees $d(s), d(t)$ in it, which is favorable particularly for graphs with high average degrees. The empirical results in Section 5.4 reveal the great superiority of our refined ℓ over Peng et al.'s ℓ in the practical efficiency of PER computation. Given that \mathbf{P} is a sparse matrix with m non-zero entries, iterative methods [21] such as the Implicitly Restarted Arnoldi Method [37] for computing λ merely require performing sparse matrix-vector multiplications between \mathbf{P} and two length- n vectors, resulting in linear time complexity of $O(m)$. This suggests that the computation of λ can be efficiently done through a preprocessing step. For example, on the Orkut graph with 117 million edges, computing λ consumes less than five minutes. Note that this preprocessing step only needs to be conducted once for a graph, and the obtained λ can be reused for computing the maximum length ℓ by Eq. (6) for any node pairs.

3.2 Sampling Random Walks Adaptively

Before delving into the algorithmic details, we first elaborate on the high-level idea of AMC.

3.2.1 High-level Idea. Recall from Section 2.3 that TP and TPC utilize the Hoeffding's inequality (Lemma 2.3) to derive the maximum number of random walks needed in advance before conducting them in a single batch. Practically, most of the random walks are excessive due to the looseness of the Hoeffding bound, wherein the actual variance of random variables is much lower than the one it assumes. Ideally, an efficient method should run with the minimum amount of random walks derived according to the actual variance, which is unknown beforehand.

Motivated by this, AMC's idea is to alter the sampling phase such that it runs adaptively. That is, instead of performing all random walks in a single batch, we conduct multiple batches of independent Monte Carlo random walks incrementally to estimate ER $r(s, t)$, and determine the termination according to the empirical error computed from the observed samples. Note that the empirical error can be calculated via the empirical Bernstein inequality in Lemma 3.2. Fig. 1 overviews this adaptive sampling scheme adopted in AMC. More specifically, AMC starts with a small-size batch of random walks (η samples in total) to compute an approximate ER $r'(s, t)$. Let η^* be the maximum number of random walks required by Lemma 2.3. If either η exceeds η^* or the empirical error $f(\eta, \hat{\sigma}^2, \psi, \delta)$ computed by Lemma 3.2 is not greater than the desired error threshold $\epsilon/2$, AMC terminates and returns $r'(s, t)$ as the answer. Otherwise, we discard all results and samples

Algorithm 1: AMC

Input: Graph G , two nodes s, t , two vectors \vec{s}, \vec{t} , error threshold ϵ , maximum random walk length ℓ_f , the number τ of batches, and failure probability δ

Output: $r_f(s, t)$

```

1  Compute  $\eta^*$  by Eq. (8) and  $\psi$  by Eq. (9);
2   $\eta \leftarrow \lceil \eta^* / 2^{\tau-1} \rceil$ ;
3  for  $i \leftarrow 1$  to  $\tau$  do
4       $Z \leftarrow 0$ ;  $\hat{\sigma}^2 \leftarrow 0$ ;
5      for  $k \leftarrow 1$  to  $\eta$  do
6          Perform two random walks  $S_k$  and  $T_k$  with length- $\ell_f$  from  $s$  and  $t$ , respectively;
7           $Z_k \leftarrow \sum_{u \in S_k} \left( \frac{\vec{s}(u)}{d(s)} - \frac{\vec{t}(u)}{d(t)} \right) + \sum_{u \in T_k} \left( \frac{\vec{t}(u)}{d(t)} - \frac{\vec{s}(u)}{d(s)} \right)$ ;
8          Update  $Z \leftarrow Z + Z_k$ ;
9          Update  $\hat{\sigma}^2 \leftarrow \hat{\sigma}^2 + Z_k^2$ ;
10     end
11     Compute  $Z \leftarrow \frac{Z}{\eta}$ ;
12     Compute  $\hat{\sigma}^2 \leftarrow \frac{\hat{\sigma}^2}{\eta} - Z^2$ ;
13     if  $f(\eta, \hat{\sigma}^2, \psi, \delta/\tau) \leq \frac{\epsilon}{2}$  then break;
14      $\eta \leftarrow 2\eta$ ;
15 end
16 return  $r_f(s, t) \leftarrow Z$ ;

```

in this batch and repeat the above procedure with an increased η . This adaptive scheme ensures its cost never exceeds that of simple Monte Carlo by imposing a restriction on η , i.e., $\eta \leq \eta^*$. On top of that, it largely curtails the amount of random walks in AMC compared with prior Monte Carlo approaches (e.g., TP) as the experiments in Section 5 demonstrate, owing to that the empirical Bernstein inequality quickly gets to be much tighter than the Hoeffding's inequality when the variances of the random variables are small [44].

LEMMA 3.2 (EMPIRICAL BERNSTEIN INEQUALITY [6]). *Let Z_1, Z_2, \dots, Z_{n_z} be real-valued i.i.d. random variables, such that $0 \leq Z_i \leq \psi$. We denote by $Z = \frac{1}{n_z} \sum_{i=1}^{n_z} Z_i$ the empirical mean of these variables and $\hat{\sigma}^2 = \frac{1}{n_z} \sum_{i=1}^{n_z} (Z_i - Z)^2$ their empirical variance. Then, we have*

$$\mathbb{P} \left[|Z - \mathbb{E}[Z]| \geq f(n_z, \hat{\sigma}^2, \psi, \delta) \right] \leq \delta,$$

where

$$f(n_z, \hat{\sigma}^2, \psi, \delta) = \sqrt{\frac{2\hat{\sigma}^2 \log(3/\delta)}{n_z}} + \frac{3\psi \log(3/\delta)}{n_z}. \quad (7)$$

Building on the idea explained above, we delineate the algorithmic details of AMC in what follows.

3.2.2 Algorithm. Algorithm 1 illustrates the pseudo-code of AMC. To begin with, AMC takes as input a graph G , two nodes s, t , maximum random walk length ℓ_f , the error threshold ϵ , failure probability δ , the number of batches τ , and two length- n non-negative vectors \vec{s} and \vec{t} . For the case of ϵ -approximate PER computation, \vec{s} (resp. \vec{t}) is fixed to be \vec{e}_s (resp. \vec{e}_t), as explained later in Section 3.3. Initially, AMC computes the maximum number η^* of random walks required from both s

and t and a parameter ψ at Line 1 by the following equations:

$$\eta^* = \frac{2\psi^2 \log(2\tau/\delta)}{\epsilon^2}, \quad (8)$$

where

$$\psi = 2 \left\lceil \frac{\ell_f}{2} \right\rceil \left(\frac{\max_1(\vec{s})}{d(s)} + \frac{\max_1(\vec{t})}{d(t)} \right) + 2 \left\lfloor \frac{\ell_f}{2} \right\rfloor \left(\frac{\max_2(\vec{s})}{d(s)} + \frac{\max_2(\vec{t})}{d(t)} \right). \quad (9)$$

Intuitively, the parameter $\psi/2$ can be regarded as an upper bound for the absolute value of the random variable sampled by each random walk in AMC (detailed in Section 3.3). AMC then initializes the number η of random walks to be performed from both s and t as $\lceil \eta^*/2^{\tau-1} \rceil$ (Line 2). Afterwards, AMC starts τ batches of sampling (Lines 3–14), in each i -th of which it calculates the empirical mean Z and empirical variance $\hat{\sigma}^2$, respectively. Observing that the empirical variance $\hat{\sigma}^2$ can be rewritten as

$$\hat{\sigma}^2 = \frac{1}{\eta} \sum_{k=1}^{\eta} (Z_k - Z)^2 = \frac{\sum_{k=1}^{\eta} Z_k^2}{\eta} - Z^2,$$

we can compute $\hat{\sigma}^2$ efficiently (Lines 9 and 12). We repeat the process until they satisfy any of the two termination conditions: (i) the maximum number of iterations is reached (i.e., the maximum number of required random walks are conducted) (Lines 3) and (ii) the empirical error is less than the desired error threshold $\frac{\epsilon}{2}$ (Line 13). Finally, $r_f(s, t) = Z$ will be returned to derive an accurate estimate of $r(s, t)$ (Line 16).

3.3 Analysis

In what follows, we theoretically analyze the correctness and complexity of AMC.

3.3.1 Correctness. In the following, we will show that $r_f(s, t) + \mathbb{1}_{s \neq t} \cdot (\frac{1}{d(s)} + \frac{1}{d(t)})$ is an ϵ -approximation of $r(s, t)$ (Eq. (2)) w.h.p. when the input $\ell_f = \ell$ (Eq. (6)), $\vec{s} = \vec{e}_s$ and $\vec{t} = \vec{e}_t$.

LEMMA 3.3. *Given a length- n non-negative vector \vec{x} and any length- ℓ_f random walk W originating from u on graph G , we have*

$$\ell_f \cdot \min(\vec{x}) \leq \sum_{w \in W} \vec{x}(w) \leq \left\lceil \frac{\ell_f}{2} \right\rceil \cdot \max_1(\vec{x}) + \left\lfloor \frac{\ell_f}{2} \right\rfloor \cdot \max_2(\vec{x}). \quad (10)$$

For random walks S_k and T_k with length- ℓ_f (Line 6), consider the random variable Z_k arising from the random walk in AMC (Line 7) such that

$$Z_k = \sum_{u \in S_k} \left(\frac{\vec{s}(u)}{d(s)} - \frac{\vec{t}(u)}{d(t)} \right) + \sum_{u \in T_k} \left(\frac{\vec{t}(u)}{d(t)} - \frac{\vec{s}(u)}{d(s)} \right). \quad (11)$$

By Lemma 3.3, given $\min(\vec{s}) \geq 0$ and $\min(\vec{t}) \geq 0$, we have

$$|Z_k| \leq \left\lceil \frac{\ell_f}{2} \right\rceil \left(\frac{\max_1(\vec{s})}{d(s)} + \frac{\max_1(\vec{t})}{d(t)} \right) + \left\lfloor \frac{\ell_f}{2} \right\rfloor \left(\frac{\max_2(\vec{s})}{d(s)} + \frac{\max_2(\vec{t})}{d(t)} \right) = \frac{\psi}{2},$$

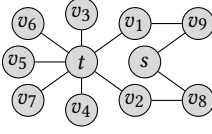
where ψ is given in Eq. (9). Further, let

$$q(s, t) := \sum_{i=1}^{\ell_f} \sum_{v \in V} \left((p_i(s, v) - p_i(t, v)) \cdot \left(\frac{\vec{s}(v)}{d(s)} - \frac{\vec{t}(v)}{d(t)} \right) \right), \quad (12)$$

where $p_i(s, v)$ (resp. $p_i(t, v)$) signifies the probability that a length- i random walk starting from node s (resp. t) would end at node v . Then, by the definition of Z_k (Line 7), it is trivial to derive the expectation of Z_k as follows:

$$\mathbb{E}[Z_k] = q(s, t), \quad (13)$$

which indicates that $r_f(s, t) = Z$ (Line 16) is an unbiased estimator of $q(s, t)$.



ℓ_f	1	2	3	4	5	6	7	8
#path(s)	2	4	8	26	42	184	268	1346
#path(t)	7	9	53	71	397	539	2963	4041
#path(s) + #path(t)	9	13	61	97	439	723	3231	5387
η^*	31	122	275	488	762	1097	1493	1949

Fig. 2. A running example.

Note that Algorithm 1 terminates under two conditions: (i) $\epsilon_f \leq \frac{\epsilon}{2}$, where $\epsilon_f = f(\eta, \hat{\sigma}^2, \psi, \delta/\tau)$ (Line 13), or (ii) $\eta \geq \eta^*$ (Line 3). For the first case that $\epsilon_f \leq \frac{\epsilon}{2}$, we can bound its failure probability by applying the empirical Bernstein inequality (Lemma 3.2). As for another termination case that $\eta \geq \eta^*$, its failure probability can be bounded by using Hoeffding's inequality (Lemma 2.3). Further, using union bound over these two cases, we can prove $r_f(s, t)$ returned by Algorithm 1 is an $\frac{\epsilon}{2}$ -approximate of $q(s, t)$ with high probability. In addition, note that $r_\ell(s, t) = q(s, t) + \mathbb{1}_{s \neq t} \cdot (\frac{1}{d(s)} + \frac{1}{d(t)})$ when the input of Algorithm 1 satisfies $\ell_f = \ell$ as in Eq. (6), $\vec{s} = \vec{e}_s$ and $\vec{t} = \vec{e}_t$. Therefore, in Theorem 3.4, we have $\left| r_f(s, t) + \mathbb{1}_{s \neq t} \cdot \left(\frac{1}{d(s)} + \frac{1}{d(t)} \right) - r_\ell(s, t) \right| \leq \frac{\epsilon}{2}$ with high probability; in other words, $r_f(s, t) + \mathbb{1}_{s \neq t} \cdot \left(\frac{1}{d(s)} + \frac{1}{d(t)} \right)$ is an ϵ -approximate ER of node pair (s, t) .

THEOREM 3.4. *Algorithm 1 ensures $|r_f(s, t) - q(s, t)| \leq \frac{\epsilon}{2}$ with a probability of at least $1 - \delta$. Moreover, setting $\ell_f = \ell$ as in Eq. (6), $\vec{s} = \vec{e}_s$ and $\vec{t} = \vec{e}_t$, Algorithm 1 returns $r_f(s, t)$ satisfying $\left| r_f(s, t) + \mathbb{1}_{s \neq t} \cdot \left(\frac{1}{d(s)} + \frac{1}{d(t)} \right) - r(s, t) \right| \leq \epsilon$ with a probability of at least $1 - \delta$.*

3.3.2 Complexity. According to Lines 2 and 14 in Algorithm 1, the total number of random walks conducted from nodes s, t in the course of τ iterations is bounded by

$$h(\ell_f) = \sum_{i=1}^{\tau} 2^{i-1} \eta = (2^\tau - 1) \eta < 2\eta^*.$$

The running time of AMC is bounded by $O(h(\ell_f) \cdot \ell_f)$ as the length of each random walk in AMC is ℓ_f . When $\ell_f = \ell$ (Eq. (6)), $\vec{s} = \vec{e}_s$, $\vec{t} = \vec{e}_t$, Eq. (9) implies $\psi = 2 \lceil \frac{\ell}{2} \rceil \left(\frac{1}{d(s)} + \frac{1}{d(t)} \right)$. Recall that η^* is defined in Eq. (8). Therefore, the total time complexity of employing AMC for answering ϵ -approximate PER query of node pair (s, t) is

$$O\left(\left(\frac{1}{\epsilon d(s)} + \frac{1}{\epsilon d(t)}\right)^2 \log^3\left(\frac{1}{\epsilon d(s)} + \frac{1}{\epsilon d(t)}\right)\right) = O\left(\frac{1}{\epsilon^2 d^2} \log^3\left(\frac{1}{\epsilon d}\right)\right), \quad (14)$$

where $d = \min\{d(s), d(t)\}$ and δ is regarded as a constant.

Remark. The total number of random walks conducted in AMC for answering an ϵ -approximate PER query is roughly $\frac{2\ell^2 \log(2\tau/\delta)}{\epsilon^2} \cdot \left(\frac{1}{d(s)} + \frac{1}{d(t)}\right)^2$. By contrast, the state of the art PER solution TP requires $\frac{40\ell^3 \ln(8\ell/\delta)}{\epsilon^2}$ random walks [49], which is larger than AMC's amount by at least a significant factor of $20\ell / \left(\frac{1}{d(s)} + \frac{1}{d(t)}\right)^2$.

4 THE GREEDY APPROACH

Although AMC significantly improves over existing approaches in terms of running time, we observe in our experiments (Section 5) that the performance of AMC is still intolerable especially for large graphs, as an aftermath of the enormous number of excessive random walks needed in it. To explain,

we illustrate an example in Fig. 2, which contains a toy graph with eleven nodes including v_1-v_9 and s, t .

A Running Example. The r.h.s. table in Fig. 2 lists the numbers $\#path(s), \#path(t)$ of distinct paths from node s and t within varied length ℓ_f (ranging from 1 to 8). Note that these numbers can be obtained by performing deterministic graph traversals from nodes s and t , and used to compute $r_f(s, t)$. The table also reports η^* , which is the number of random walks required by AMC from nodes s and t to estimate $r_f(s, t)$ when varying length ℓ_f from 1 to 8 with additive error $\epsilon = 0.5$ and failure probability $\delta = 0.1$. As we can see from the table, when length ℓ_f is increased from 1 to 8, η^* constantly outnumbers $\#path(s) + \#path(t)$ by up to 10-fold, whereas $\#path(t) + \#path(t)$ exceeds η^* notably when $\ell_f \geq 7$. The former is by virtue of the insignificant amount of nodes in the near vicinity of nodes s and t , and thus a simple graph traversal can efficiently explore all of them. This suggests that AMC tends to be even less efficient than the deterministic graph traversal, when ℓ_f is small and source nodes have scant connections to the rest of the graph. However, as ℓ_f continues to increase, the number $\#path(t)$ of paths from t grows at an astonishing rate (from 7 to 4041) as it has 7 adjacent neighbors, rendering sampling random walks (i.e., AMC) a preferred choice over the graph traversal. This happens especially on large graphs with high average degrees.

Based upon the above-said observations, it is natural to investigate how to combine AMC and deterministic graph traversal together and create an even more efficient approach for answering ϵ -approximate PER queries. To achieve this goal, this section proposes GEER (Greedy Estimation of Effective Resistance), which significantly advances the practical efficiency of AMC without degrading its theoretical guarantees, by harnessing the virtues of sparse matrix-vector multiplications and random walks in a judicious manner. The subsequent section elucidates the rationale behind GEER; after that the detailed algorithm and rigorous theoretical analysis will be presented.

4.1 Overview of GEER

To begin with, we introduce a secondary algorithm SMM, which implements the deterministic graph traversal over G based on sparse matrix-vector multiplications.

4.1.1 A Deterministic Method SMM. Recall from Eq. (4) that the computation of $r_\ell(s, t)$ involves calculating $p_i(s, t)$, $p_i(s, s)$ and $p_i(t, t)$ for $0 \leq i \leq \ell$. By definition, for any two nodes $u, v \in V$

$$p_i(v, u) = \mathbf{P}^i(v, u) = (\mathbf{P}^i \vec{\mathbf{e}}_u)(v) = (\underbrace{\mathbf{P} \cdot \mathbf{P} \cdots \mathbf{P}}_{i \text{ times}} \cdot \vec{\mathbf{e}}_u)(v),$$

and $p_0(u, v) = \vec{\mathbf{e}}_u(v)$. Therefore, $r_\ell(s, t)$ can be obtained via an iterative process of sparse matrix-vector multiplications as displayed in Algorithm 2 with initial vectors $\vec{\mathbf{s}}^* = \vec{\mathbf{e}}_s$, $\vec{\mathbf{t}}^* = \vec{\mathbf{e}}_t$, and

$$r_b(s, t) = \frac{\vec{\mathbf{s}}^*(s)}{d(s)} + \frac{\vec{\mathbf{t}}^*(t)}{d(t)} - \frac{\vec{\mathbf{s}}^*(t)}{d(s)} - \frac{\vec{\mathbf{t}}^*(s)}{d(t)},$$

where $r_b(s, t)$ is equal to $\frac{p_0(s, s)}{d(s)} + \frac{p_0(t, t)}{d(t)} - \frac{p_0(s, t)}{d(s)} - \frac{p_0(t, s)}{d(t)}$, i.e., the zeroth iteration part of $r_\ell(s, t)$.

Each of the ℓ_b iterations in SMM updates $\vec{\mathbf{s}}^*$ (resp. $\vec{\mathbf{t}}^*$) as $\mathbf{P}\vec{\mathbf{s}}^*$ (resp. $\mathbf{P}\vec{\mathbf{t}}^*$), and then increases $r_b(s, t)$ by $\frac{\vec{\mathbf{s}}^*(s)}{d(s)} + \frac{\vec{\mathbf{t}}^*(t)}{d(t)} - \frac{\vec{\mathbf{s}}^*(t)}{d(s)} - \frac{\vec{\mathbf{t}}^*(s)}{d(t)}$ (Lines 4–5). Particularly, at the end of the i -th iteration, $\forall v \in V$,

$$\vec{\mathbf{s}}^*(v) = p_i(v, s), \text{ and } \vec{\mathbf{t}}^*(v) = p_i(v, t). \quad (15)$$

In turn, when $\ell_b = \ell$ (as defined in Eq. (6)), the $r_b(s, t)$ returned by SMM is an approximation of $r(s, t)$ satisfying $|r(s, t) - r_\ell(s, t)| \leq \frac{\epsilon}{2}$.

SMM is essentially a deterministic graph traversal over G . Compared to naïve graph traversal, SMM attains cache-friendly memory access patterns as it sequentially visits all reachable nodes from node s, t via $\mathbf{P}\vec{\mathbf{s}}^*$ and $\mathbf{P}\vec{\mathbf{t}}^*$. Recall that G is connected, meaning every two nodes can reach

Algorithm 2: SMM**Input:** Graph G , nodes s, t , ℓ_b .**Output:** $r_b(s, t)$

```

1  $\vec{s}^* \leftarrow \vec{e}_s; \vec{t}^* \leftarrow \vec{e}_t;$ 
2  $r_b(s, t) \leftarrow \frac{\vec{s}^*(s)}{d(s)} + \frac{\vec{t}^*(t)}{d(t)} - \frac{\vec{s}^*(t)}{d(s)} - \frac{\vec{t}^*(s)}{d(t)};$ 
3 for  $i \leftarrow 1$  to  $\ell_b$  do
4    $\vec{s}^* \leftarrow P\vec{s}^*; \vec{t}^* \leftarrow P\vec{t}^*;$ 
5    $r_b(s, t) \leftarrow r_b(s, t) + \frac{\vec{s}^*(s)}{d(s)} + \frac{\vec{t}^*(t)}{d(t)} - \frac{\vec{s}^*(t)}{d(s)} - \frac{\vec{t}^*(s)}{d(t)};$ 
6 end

```

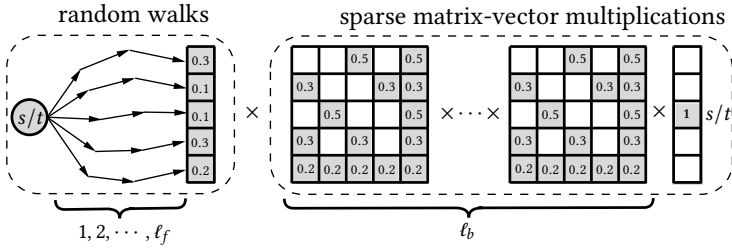


Fig. 3. Overview of GEER

each other via one or multiple paths. Thus, when ℓ_b is sufficiently large and source nodes s, t have many neighbors, the vectors \vec{s}^* and \vec{t}^* in SMM turns to be dense rapidly and during each iteration in Algorithm 2, the matrix-vector multiplications at Line 4 will consume an exorbitant time of up to $O(m)$.

With the strengths and weaknesses of AMC and SMM in mind, next we investigate how to integrate them into GEER, as well as orchestrate and optimize the entire GEER algorithm for enhanced empirical efficiency.

4.1.2 Greedy Integration of SMM and AMC. Fig. 3 depicts an overview of our proposed GEER. At a high level, GEER is to strike a good trade-off between ℓ_b ($\ell_b \leq \ell$) iterations of sparse matrix-vector multiplications in SMM and random walks in AMC. More precisely, GEER aims to compute $r_b^*(s, t)$ and $r_f^*(s, t)$ as follows:

$$\begin{aligned}
 r_b^*(s, t) &= \sum_{i=0}^{\ell_b} \frac{p_i(s, s)}{d(s)} + \frac{p_i(t, t)}{d(t)} - \frac{p_i(s, t)}{d(t)} - \frac{p_i(t, s)}{d(s)}, \\
 r_f^*(s, t) &= \sum_{i=\ell_b+1}^{\ell} \frac{p_i(s, s)}{d(s)} + \frac{p_i(t, t)}{d(t)} - \frac{p_i(s, t)}{d(t)} - \frac{p_i(t, s)}{d(s)},
 \end{aligned} \tag{16}$$

and finally combine them as the final ER via $r_\ell(s, t) = r_b^*(s, t) + r_f^*(s, t)$. Note that $r_b^*(s, t)$ aggregates the probabilities of visiting all nodes within the vicinity of ℓ_b hops away from nodes s, t , which can be efficiently computed using SMM when ℓ_b is small, as remarked earlier. As regards $r_f^*(s, t)$, given that it considers far-reaching nodes beyond ℓ_b hops from s, t , we resort to conducting random walks described in AMC to estimate it. Instead of simulating random walks of lengths ranging from $\ell_b + 1$ to ℓ , we leverage the byproduct in SMM so as to reduce the length as well as the amount of random walks needed in AMC, as stated in what follows.

Let \vec{s}^* and \vec{t}^* be the vectors after ℓ_b iterations in SMM. By Eq. (15), we have $\vec{s}^*(v) = p_{\ell_b}(v, s)$ and $\vec{t}^*(v) = p_{\ell_b}(v, t) \forall v \in V$. As a consequence, $r_f^*(s, t)$ in Eq. (16) can be rewritten as follows:

$$\begin{aligned} r_f^*(s, t) &= \sum_{i=1}^{\ell-\ell_b} \frac{\sum_{v \in V} p_i(s, v) \cdot p_{\ell_b}(v, s)}{d(s)} + \frac{\sum_{v \in V} p_i(t, v) \cdot p_{\ell_b}(v, t)}{d(t)} \\ &\quad - \frac{\sum_{v \in V} p_i(s, v) \cdot p_{\ell_b}(v, t)}{d(t)} - \frac{\sum_{v \in V} p_i(t, v) \cdot p_{\ell_b}(v, s)}{d(s)} \\ &= \sum_{i=1}^{\ell-\ell_b} \sum_{v \in V} \left((p_i(s, v) - p_i(t, v)) \cdot \left(\frac{\vec{s}^*(v)}{d(s)} - \frac{\vec{t}^*(v)}{d(t)} \right) \right). \end{aligned}$$

Observe that the above equation is identical to $q(s, t)$ in Eq. (12) by letting $\ell_f = \ell - \ell_b$, $\vec{s} = \vec{s}^*$, and $\vec{t} = \vec{t}^*$. Namely, we can directly estimate $r_f^*(s, t)$ by invoking AMC with $\ell_f = \ell - \ell_b$, $\vec{s} = \vec{s}^*$, and $\vec{t} = \vec{t}^*$. By doing so, the length of random walks varies from 1 to $\ell - \ell_b$, rather than from $\ell_b + 1$ to ℓ .

Furthermore, a vital benefit from the intermediate result \vec{s}^* and \vec{t}^* is that we can significantly prune the random walks needed in AMC. Specifically, recall that in Eq. (8), the total number of random walks simulated in AMC is proportional to ψ^2 defined in Eq. (9). In Section 3, we input $\vec{s} = \vec{e}_s$ and $\vec{t} = \vec{e}_t$ to AMC; and thus $\psi = 2 \lceil \frac{\ell}{2} \rceil \left(\frac{1}{d(s)} + \frac{1}{d(t)} \right)$. By contrast, GEER invokes AMC with $\vec{s} = \vec{s}^*$ and $\vec{t} = \vec{t}^*$, whose maximum values will dwindle to small ones when increasing ℓ_b since they are the probabilities of length- ℓ_b random walks from a node visiting s and t . Empirically, when ℓ_b is sufficiently large, the maximum element in \vec{s}^* or \vec{t}^* is typically less than 0.2, and hence $\psi \approx \frac{2}{5} \lceil \frac{\ell}{2} \rceil \left(\frac{1}{d(s)} + \frac{1}{d(t)} \right)$, yielding at least a 96% reduction in the amount of random walks in AMC. Additionally, with $\vec{s} = \vec{s}^*$ and $\vec{t} = \vec{t}^*$ as input to AMC, the variance $\hat{\sigma}^2$ in AMC can be considerably narrowed, thereby facilitating the early termination of AMC (at Line 13 in Algorithm 1). To see this, we first recall that the random variable Z_k in AMC is the weighted sums of ℓ_f entries in \vec{s} or \vec{t} . In GEER, entries in \vec{s}^* (resp. \vec{t}^*) are more evenly distributed compared to \vec{e}_s (resp. \vec{e}_t), resulting in smaller variance $\hat{\sigma}^2$. In sum, we can tremendously expedite the computational efficiency of AMC by picking a large ℓ_b , which ensures the maximum values in \vec{s}^* and \vec{t}^* are small and values in them are evenly distributed.

To minimize the total cost incurred by GEER, we adopt a greedy strategy to determine ℓ_b , i.e., the switch point between SMM and AMC. In a nutshell, we cease the iterative sparse matrix-vector multiplications (SMM) and start to simulate random walks (AMC) once the overhead of the former exceeds that of the latter. To be specific, consider ℓ_b -th iteration in SMM. Let V_s and V_t be the sets of nodes having non-zero entries in \vec{s} and \vec{t} , respectively. Intuitively, the total number of operations when performing $\vec{P}\vec{s}$ and $\vec{P}\vec{t}$ in the following iteration is bounded by $\sum_{v \in V_s} d(v) + \sum_{v \in V_t} d(v)$. On the other hand, the total number of random samples required in AMC is currently $h(\ell - \ell_b)$. Thus, GEER greedily performs sparse matrix-vector multiplications as in SMM until the following inequality holds.

$$\sum_{v \in V_s} d(v) + \sum_{v \in V_t} d(v) > h(\ell - \ell_b). \quad (17)$$

4.2 Complete GEER Algorithm and Analysis

The complete pseudo-code of GEER is presented in Algorithm 3. Algorithm 3 starts by taking as input a graph G , two nodes s, t , the error threshold ϵ , the number of batches τ , and the failure probability δ . First, GEER calculates ℓ according to Eq. (6) (Line 1). We assume that λ in Eq. (6) is

Algorithm 3: GEER

Input: Graph G , nodes s, t , error threshold ϵ , the maximum number τ of batches in AMC, failure probability δ

Output: $r'(s, t)$

```

1 Calculate  $\ell$  according to Eq. (6);
2  $\ell_b \leftarrow 0$ ;
3  $\vec{s}^* \leftarrow \vec{e}_s; \vec{t}^* \leftarrow \vec{e}_t$ ;
4  $r_b(s, t) \leftarrow \frac{\vec{s}^*(s)}{d(s)} + \frac{\vec{t}^*(t)}{d(t)} - \frac{\vec{s}^*(t)}{d(s)} - \frac{\vec{t}^*(s)}{d(t)}$ ;
5 repeat
6    $\vec{s}^* \leftarrow \mathbf{P}\vec{s}^*; \vec{t}^* \leftarrow \mathbf{P}\vec{t}^*$ ;
7    $r_b(s, t) \leftarrow r_b(s, t) + \frac{\vec{s}^*(s)}{d(s)} + \frac{\vec{t}^*(t)}{d(t)} - \frac{\vec{s}^*(t)}{d(s)} - \frac{\vec{t}^*(s)}{d(t)}$ ;
8    $\ell_b \leftarrow \ell_b + 1$ ;
9 until Eq. (17) holds or  $\ell_b \geq \ell$ ;
10  $r_f(s, t) \leftarrow \text{AMC}(G, s, t, \vec{s}^*, \vec{t}^*, \epsilon, \ell - \ell_b, \tau, \delta)$ ;
11  $r'(s, t) \leftarrow r_f(s, t) + r_b(s, t)$ ;

```

obtained in a pre-processing step. Then, GEER initializes $\ell_b = 0$ (Line 2) and starts to invoke SMM (Lines 3–9). Distinct from SMM, the iterative procedure is terminated when Eq. (17) holds (Line 9) or the number ℓ_b of iterations performed thus far exceeds ℓ (i.e., $\ell_b \geq \ell$). After that, Algorithm 1 is invoked with parameters $G, s, t, \epsilon, \delta, \vec{s}^*, \vec{t}^*$, and $\ell_f = \ell - \ell_b$ (Line 10). Let $r_f(s, t)$ be the output of AMC. Eventually, GEER computes $r'(s, t)$ by $r'(s, t) = r_f(s, t) + r_b(s, t)$ and return it as an ϵ -approximate ER of node pair (s, t) (Lines 10–11). According to Theorem 3.4, $|r_f(s, t) - r_f^*(s, t)| \leq \frac{\epsilon}{2}$ holds with probability at least $1 - \delta$. With $r_b(s, t) = r_b^*(s, t)$ as defined in Eq. (16), we derive

$$|r'(s, t) - r_\ell(s, t)| = |r_f(s, t) + r_b(s, t) - r_f^*(s, t) - r_b^*(s, t)| \leq \frac{\epsilon}{2}.$$

Plugging it into $|r(s, t) - r_\ell(s, t)| \leq \frac{\epsilon}{2}$ leads to Ineq. (2), indicating that $r'(s, t)$ returned by Algorithm 3 is an ϵ -approximation of $r(s, t)$.

The invocation of Algorithm 1 at Line 10 requires $O(h(\ell - \ell_b) \cdot (\ell - \ell_b))$ time. Notice that we ensure the cost of each iteration in Lines 6–7 not exceed that of using AMC by Eq. (17) (Line 9). Consequently, the overall time complexity of GEER is bounded by Eq. (14) as well.

5 EXPERIMENTS

This section experimentally evaluates the efficiency and accuracy of our proposed algorithms for answering ϵ -approximate PER queries.

5.1 Experimental Setup

Datasets, Query sets, and Groundtruth. To evaluate both the efficiency and accuracy of our proposed AMC and GEER, we conduct experiments on 6 real datasets of various sizes, as described in Table 3. All datasets are collected from SNAP¹ and used as benchmark datasets in prior work [49]. For each dataset, we pick 100 node pairs uniformly at random as the random query set and randomly select 100 edges out of edge set E as the edge query set. The ground-truth ER values for these query node pairs are obtained by applying SMM with 1000 iterations in parallel (ϵ is roughly 10^{-8} – 10^{-6}).

¹<https://snap.stanford.edu>

Table 3. Statistics of Datasets

Name	#nodes (n)	#edges (m)	avg. degree
Facebook [43]	4,039	88,234	43.69
DBLP [74]	317,080	1,049,866	6.62
YouTube [74]	1,134,890	2,987,624	5.27
Orkut [74]	3,072,441	117,185,082	76.28
LiveJournal [74]	3,997,962	34,681,189	17.35
Friendster [74]	65,608,366	1,806,067,135	55.06

Implementation Details. All experiments are conducted on a Linux machine with an Intel Xeon(R) Gold 6240@2.60GHz 32-core processor and 377GB of RAM. None of the experiments need anywhere near all the memory, nor any of the parallelism. Each experiment loaded the graph used into memory before beginning any timings. The eigenvalues λ_2 and λ_n of each tested dataset are approximated via ARPACK² [37]. For a fair comparison, all tested algorithms are implemented in C++ and compiled by g++ 7.5 with -O3 optimization. For reproducibility, the source code is available at: <https://github.com/AnryYang/GEER>.

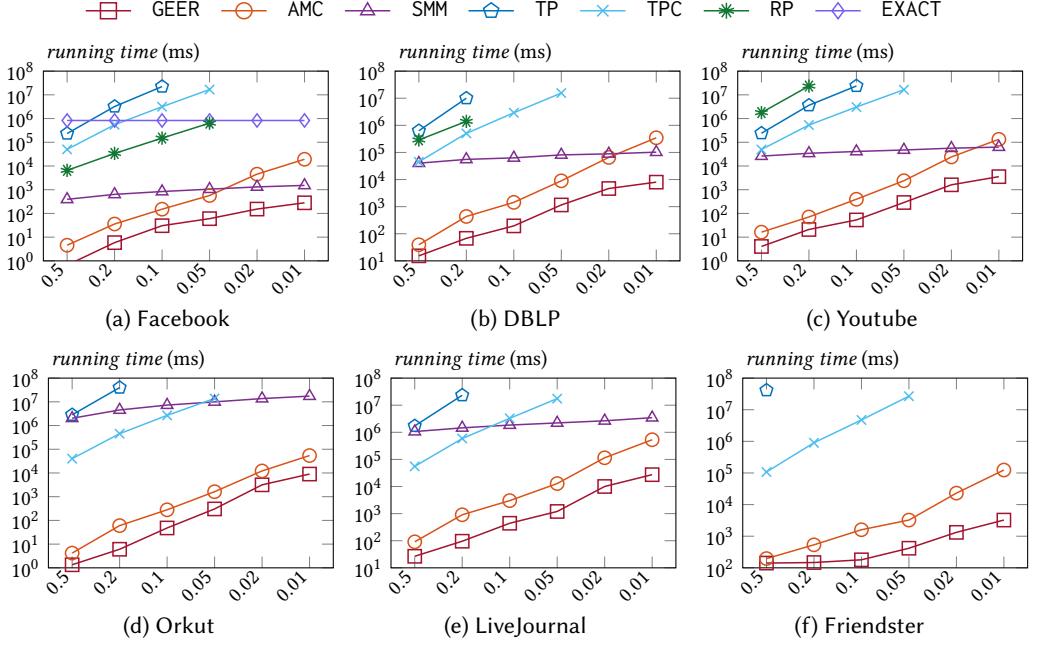
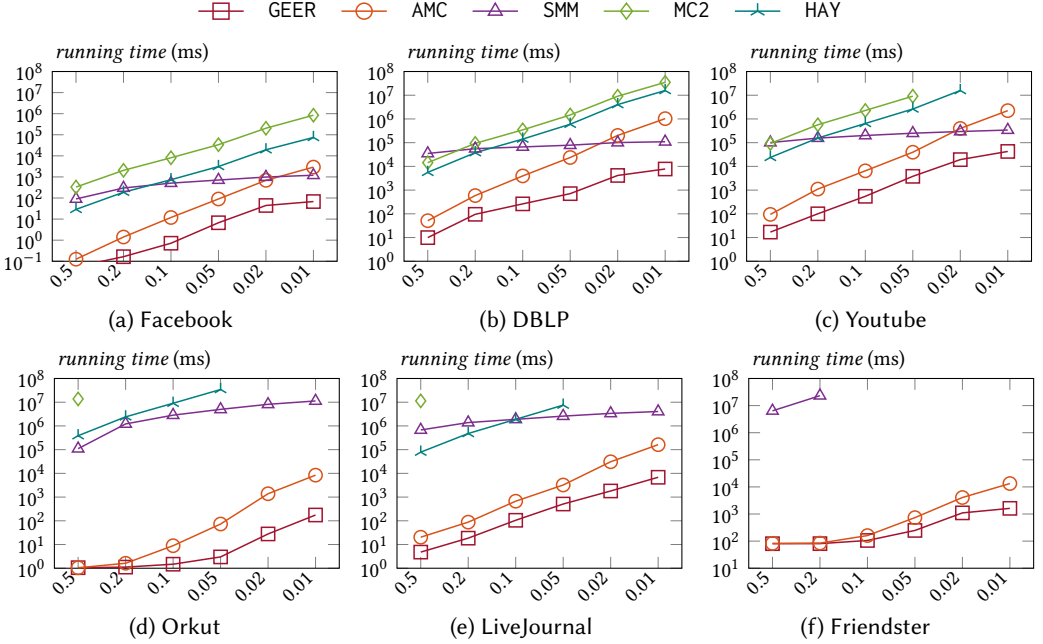
Competitors and Parameters. For random queries, we compare AMC and GEER with SMM, the state-of-the-art solutions TP and TPC discussed in Section 2.3, as well as the random projection method RP [62]. We also include the EXACT method for comparison that requires computing the pseudo-inverse of matrix $\mathbf{D} - \mathbf{A}$ in Eq. (1). For edge queries, i.e., $(s, t) \in E$, we evaluate AMC and GEER against SMM, and two baseline solutions HAY [29] and MC2 [49], which are specially designed for answering edge queries. We set the input parameter ℓ_b of SMM according to Eq. (6).

For all randomized algorithms (i.e., AMC, GEER, TP, TPC, and MC2), we set failure probability $\delta = 0.01$. Since the input parameters β_i of TPC are unknown, we adopt the heuristic settings suggested in [49]. Note that these settings do not ensure the returned value of TPC is an ϵ -approximate PER. Unless otherwise specified, the number of batches τ in AMC and GEER is set to 5. We report the average query times (measured in wall-clock time) and the actual average absolute error of each algorithm on each dataset with various ϵ in $\{0.01, 0.02, 0.05, 0.1, 0.2, 0.5\}$. We exclude a method if it fails to report the result for each query within one day.

5.2 Query Efficiency

Our first set of experiments compares AMC and GEER against SMM, TP, and TPC on random queries. Fig. 4 reports the evaluation results on query efficiency (i.e., average running time) of each method on each dataset when ϵ is varied from 0.01 to 0.5 (x -axis). Note that the y -axis is in log-scale and the measurement unit for running time is millisecond (ms). TP, TPC, and SMM cannot terminate within one day in some cases, and, thus their results are not reported. Note that EXACT can only handle the smallest dataset Facebook as it incurs out-of-memory errors on larger datasets due to the colossal space needed for materializing the $n \times n$ matrix pseudo-inverse. Akin to EXACT, RP runs out of memory on Orkut, LiveJournal, and Friendster datasets, where it requires constructing large dense random matrices. On small datasets including Facebook, DBLP, and Youtube, AMC offers remarkable speedup over TP and TPC, but is comparable or inferior to SMM when $\epsilon \leq 0.02$, whereas GEER consistently outperforms all competitors often by orders of magnitude. For instance, on Youtube, GEER is up to 37.5 \times and 6461 \times faster than AMC and SMM, respectively, and consistently achieves more than three orders of magnitude of speedup over RP, TP, and TPC.

²<http://www.caam.rice.edu/software/ARPACK>

Fig. 4. Running time vs. ϵ for random queries.Fig. 5. Running time vs. ϵ for edge queries.

Another observation we can make from Fig. 4 is that both AMC and GEER significantly outperform SMM, TP, and TPC on all large datasets including Orkut, LiveJournal, and Friendster. Notably, on such graphs, the efficiency of SMM is largely degraded on account of the highly expensive matrix-vector

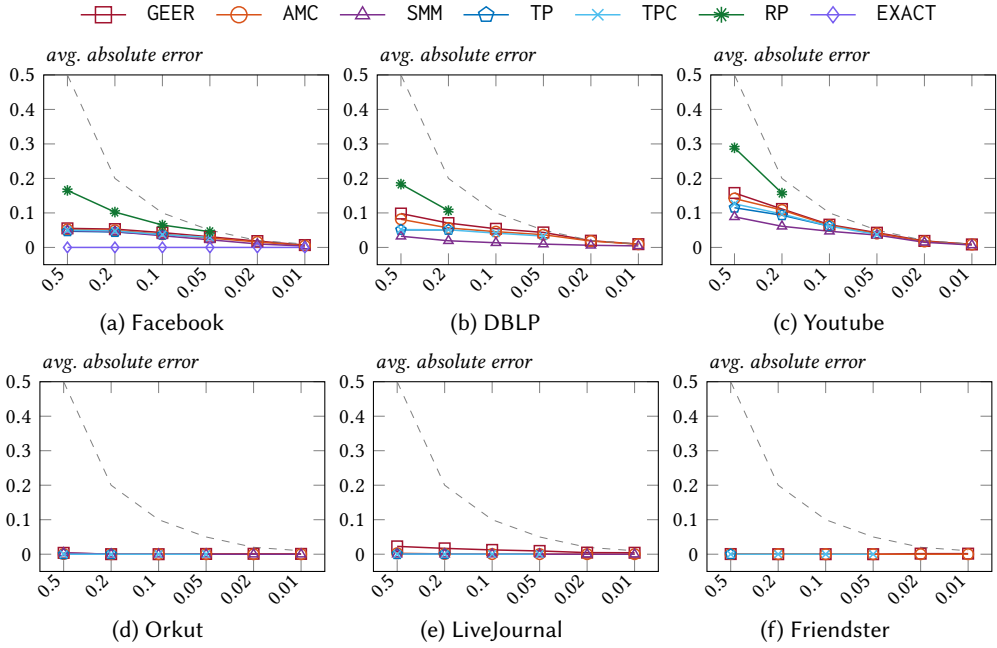


Fig. 6. Avg. absolute error vs. ϵ for random queries.

multiplications. Although AMC remarkably speeds up TP and TPC with the refined ℓ and its adaptive sampling scheme, it is still rather costly as it involves numerous random walks and intensive memory patterns on large graphs when ϵ is small. In comparison, GEER dominates all competitors including AMC with considerable speedups, i.e., up to $38.2\times$ improvement than AMC, over $126.5\times$ efficiency gain compared to SMM, as well as more than three orders of magnitude of speedup over TP, respectively. Particularly, on the billion-edge graph Friendster, given additive error $\epsilon = 0.02$, GEER finishes an ϵ -approximate PER query using only 1.3 seconds and AMC needs 23 seconds on average, whereas the rest methods are unable to finish processing within one day.

Next, we experiment with edge queries. We compare our proposed AMC and GEER with the baseline method SMM and two dedicated solutions HAY [29] and MC2 [49] for processing edge-based PER queries. Both HAY and MC2 rely on simulating a huge number of random walks without explicit length constraints. As can be seen in Fig. 5, in all cases, GEER significantly improves over the competitors in terms of query efficiency, e.g., often more than 1000-fold improvements over SMM, HAY, and MC2, and up to $132.7\times$ speed up than AMC. As for AMC, it achieves the second best performance in most cases except on small graphs including Facebook, DBLP, and Youtube when $\epsilon \leq 0.02$, where SMM has comparable or superior performance to AMC. Similar observations can be made from Fig. 4(a)–4(c). On small graphs, the vectors in SMM turn into dense ones more easily, causing slow growth in computational cost when further decreasing ϵ . Conversely, for AMC, the rising in query cost is more pronounced as ϵ reduces since the number of random walks needed in AMC (Eq. (8)) is inversely proportional to ϵ^2 .

Together these results reveal that our proposed GEER obtains high superiority in empirical efficiency over all competitors especially on large graphs with high average degrees, demonstrating the effectiveness of the greedy integration scheme developed in GEER (Section 4.1).

5.3 Query Accuracy

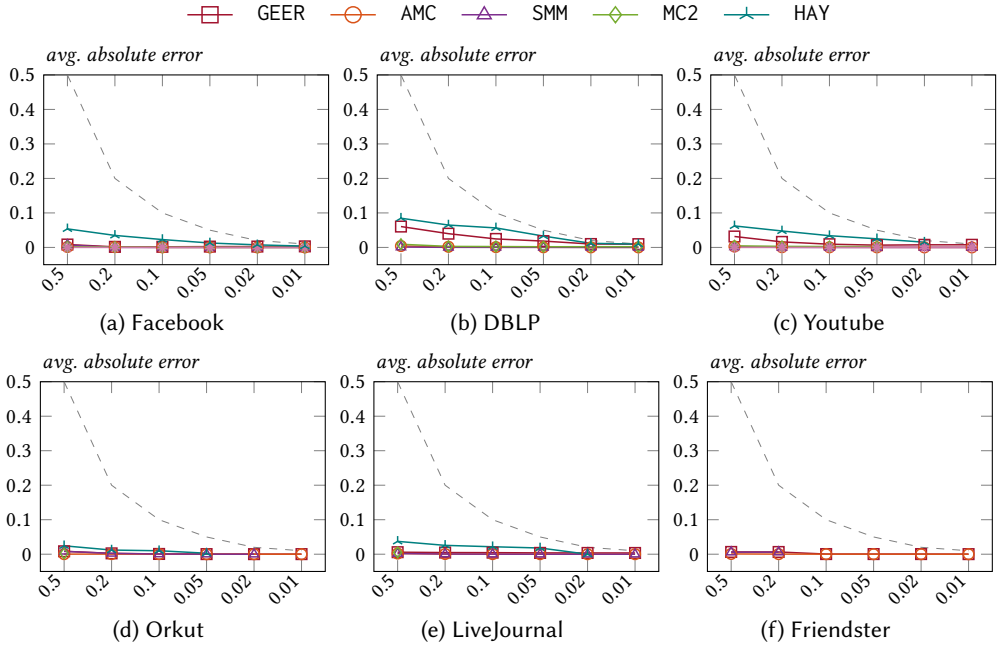
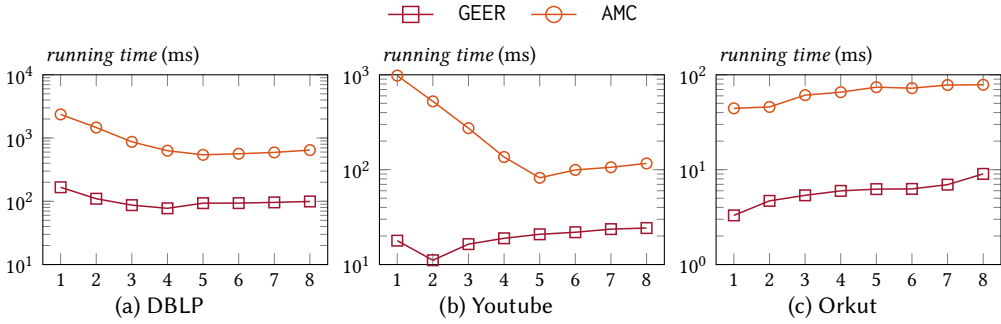
Fig. 6 and Fig. 7 report the actual average absolute error by each method on each dataset when varying ϵ from 0.01 to 0.5 for random query sets and edge query sets, respectively. Note that the x -axis and y -axis represent the given absolute error threshold ϵ and the actual average absolute error, respectively. The gray dashed line in each figure represents the boundary between successful and failed query results. That is, each data point below the line means its actual absolute error is less than the corresponding desired absolute error threshold ϵ and indicates it is a successful query result; otherwise, it is a failed query result. As observed in Fig. 6 and Fig. 7, all tested methods return accurate query results, whose actual absolute errors are less than the given error threshold ϵ . More specifically, as we can see from Fig. 6, most methods achieve low average absolute errors smaller than 0.1 for random queries even given a large error threshold $\epsilon = 0.5$ and the errors approach 0 as ϵ is lowered. In particular, the random-projection-based method RP always produces the highest empirical errors on Facebook, DBLP, and Youtube. As for GEER and AMC, they yield slightly larger errors compared to the competitors SMM, TP, and TPC on DBLP and Youtube graphs. The reason is that some of the excessive efforts made in SMM, TP, and TPC (e.g., matrix-vector multiplications or random walks) may lead to a more accurate estimation of ER, while GEER and AMC eliminate these costs as they are unnecessary. In contrast, on graphs with high average degrees, i.e., Facebook, Orkut, LiveJournal, and Friendster, GEER and AMC consistently attain insignificant errors (around 10^{-4}) as the competitors do. This is because ER $r(s, t)$ is inversely proportional to the degrees of nodes s and t , and hence the ER values as well as empirical errors in these graphs tend to be of small scale. In Fig. 7, observe that GEER, AMC, SMM, HAY, and MC2 all show similarly high accuracy for edge queries on all datasets. This is expected, since (i) the node pair of an edge (s, t) is likely to have multiple short connections to each other, making it easy to estimate accurately using random walks or graph traversals, and (ii) the ER value $r(s, t)$ (i.e., the dissimilarity between s and t) of node pair (s, t) sharing an edge is usually small.

Together with the observations in Section 5.2, we can conclude that GEER and AMC significantly improve over existing work in the practical efficiency without affecting its result quality.

5.4 Parameter Analysis

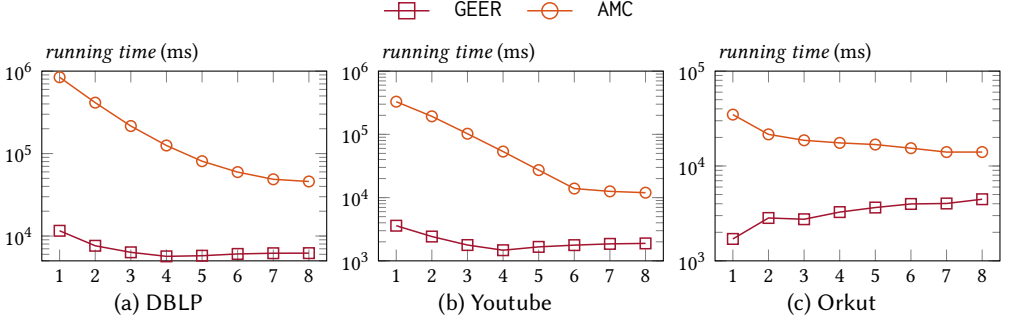
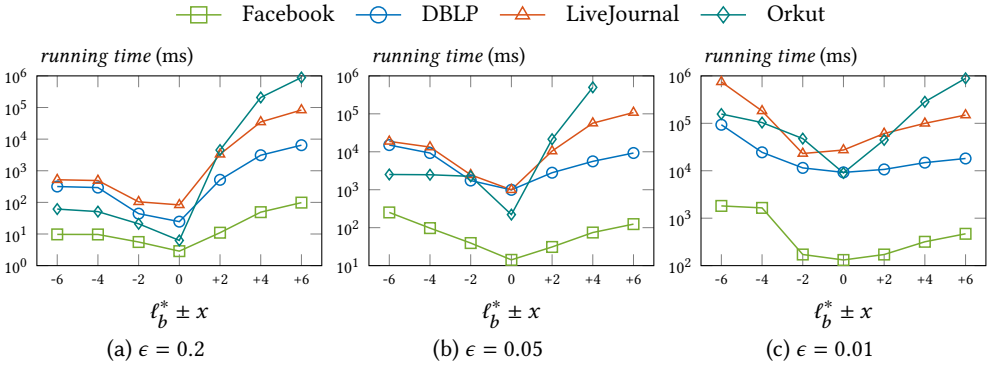
This section first studies the effect of the input parameter τ (i.e., the maximum number of batches of random walks) in AMC and GEER. Next, we vary the intermediate parameter ℓ_b in GEER so as to validate the effectiveness of the greedy strategy for combining AMC and SMM (Section 4.1.2). Lastly, we test and verify the efficiency benefits brought by our refined maximum length ℓ (Theorem 3.1) in SMM when comparing it with Peng et al.'s ℓ defined in Eq. (5).

Varying τ in AMC and GEER. Fig. 8 and Fig. 9 plot the average running times of AMC and GEER when varying τ from 1 to 8 on DBLP, Youtube, and Orkut datasets, when $\epsilon = 0.2$ and $\epsilon = 0.02$, respectively. In Fig. 8, the running times of both AMC and GEER first decrease notably and then remain stable or go up slowly as τ is increased from 1 to 8 on DBLP and Youtube. For example, on Youtube, AMC and GEER achieve the best performance when $\tau = 5$ and $\tau = 2$, which are $12\times$ and $1.6\times$ faster compared to their costs when $\tau = 1$ respectively. The result shows that a reasonable τ is conducive to averting substantial overheads incurred by random walks and facilitating early termination in AMC, which validates the effectiveness of our adaptive sampling scheme described in Section 3. We can also make similar observations from Fig. 9(a) and 9(b), where the query performance of GEER declines to a low level after τ is over 3 and the running time of AMC is drastically reduced when increasing τ from 1 to 8. This is expected, since a smaller error $\epsilon = 0.02$ will lead to immense random walks in AMC and hence more batches of random walks are needed to determine the termination point. On the Orkut dataset, the running time of GEER grows with τ as observed in Fig. 8(c) and Fig.

Fig. 7. Avg. absolute error vs. ϵ for edge queries.Fig. 8. Varying τ when $\epsilon = 0.2$.

9(c), whereas the query efficiency of AMC drops with the increase of τ when $\epsilon = 0.2$ and rises if $\epsilon = 0.02$. The reason is that Orkut has a high average degree, and thus by Eq. (14) the sampling costs in AMC and GEER are not significant. In such cases, multiple batches of sampling instead bring on additional costs. But when ϵ is small (e.g., 0.02), AMC needs numerous random walks and the adaptive sampling scheme still works. To sum up, choosing $\tau = 5$ in AMC and GEER is able to obtain appealing performance in most cases.

Varying ℓ_b in GEER. First, we denote by ℓ_b^* the value of ℓ_b determined by Eq. (17) (Line 9 in Algorithm 3). Then, we remove the requirement for Eq. (17) at Line 9 in Algorithm 3 and vary ℓ_b in the range $\{\ell_b^* - 6, \ell_b^* - 4, \ell_b^* - 2, \ell_b^*, \ell_b^* + 2, \ell_b^* + 4, \ell_b^* + 6\}$. Fig. 10 displays the average query time of GEER on four datasets (i.e., Facebook, DBLP, LiveJournal, and Orkut) when ϵ is varied from 0.01 to 0.2 and ℓ_b is varied in the above-said range. At a glance, it can be seen that GEER exhibits the best performance when ℓ_b is set to ℓ_b^* or nearly ℓ_b^* on all four datasets. More specifically, the running time of GEER first reduces considerably when increasing ℓ_b from $\ell_b^* - 6$ to ℓ_b^* and then goes up significantly as ℓ_b keeps

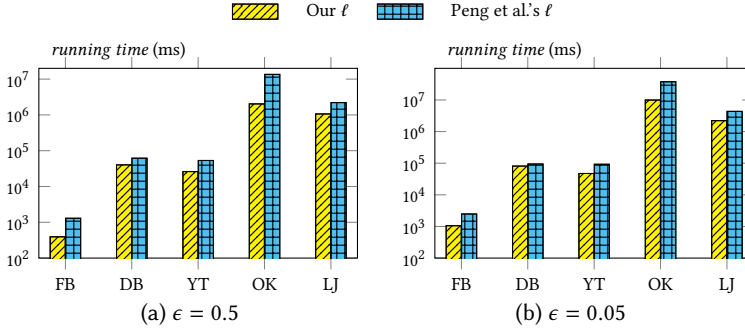
Fig. 9. Varying τ when $\epsilon = 0.02$.Fig. 10. Varying ℓ_b in GEER

increasing. For instance, on Orkut, GEER with $\ell_b = \ell_b^* \pm 6$ is orders of magnitude slower than GEER with $\ell_b = \ell_b^*$. The reasons for the remarkable changes are as follows. When ℓ_b is less than ℓ_b^* , the intermediate result $\tilde{\mathbf{s}}^*$ and $\tilde{\mathbf{t}}^*$ generated by SMM are large, and hence, GEER degrades to AMC. On the other hand, when ℓ_b is much larger than ℓ_b^* , GEER conducts vast matrix-vector multiplications that render GEER even more costly than AMC. The result shows that our greedy strategy for determining ℓ_b strikes a good balance between SMM and AMC, and enables GEER get the lowest (or nearly lowest) computation cost.

Our ℓ vs. Peng et al.'s ℓ . In the last set of experiments, we evaluate the efficiency performance of SMM (Algorithm 2) when its input parameter ℓ_b is set to our refined ℓ (Eq. (6)) and Peng et al.'s ℓ (Eq. (5)), respectively. Fig. 11 reports the average query time of SMM with two types of ℓ on five datasets including Facebook (FB), DBLP (DB), Youtube (YT), Orkut (OK), and LiveJournal (LJ). When $\epsilon = 0.5$ (Fig. 11(a)), SMM with our ℓ is $3.3\times$ and $6.7\times$ faster than SMM with Peng et al.'s ℓ on high-degree graphs FB and OK, respectively. On graphs with low average degrees (i.e., DB, YT, and LJ), our ℓ yields up to $2.1\times$ performance improvements over Peng et al.'s ℓ in SMM. This phenomenon is due to that our ℓ in Eq. (6) is inversely correlated with the degrees of query nodes, meaning that our ℓ will be much smaller than Peng et al.'s ℓ on graphs with large average node degrees. Additionally, when $\epsilon = 0.05$, our ℓ still obtains $2.4\times$ and $3.8\times$ speedups on FB and OK, respectively, and $1.2\text{--}2\times$ improvements on the remaining datasets. In sum, our refined ℓ can bring considerable efficiency enhancements to SMM compared to Peng et al.'s ℓ , especially on graphs with high average degrees.

6 ADDITIONAL RELATED WORK

In this section, we review a number of studies germane to our work.

Fig. 11. Our ℓ vs. Peng et al.'s ℓ in SMM

6.1 Effective Resistance

Apart from the methods discussed in Section 2.3 for ϵ -approximate PER queries, there exist several techniques for all pairwise ER computation or estimating ER values for all edges in the input graph, as reviewed in the sequel. Fouss et al. [24] proposed to calculate the ER value for any node pair in the input graph G by first computing the Moore-Penrose pseudoinverse of the Laplacian matrix $\mathbf{D} - \mathbf{A}$ based on a sparse Cholesky factorization of $\mathbf{D} - \mathbf{A}$. Mavroforakis et al. [42] utilized the random projection and SDD solvers to approximate the ER values of all edges. In Ref. [29], Hayashi et al. presented a method for computing approximate ER values of all edges in the input graph by sampling spanning trees. This method is still state-of-the-art for this problem. Jambulapati and Sidford then [31] introduced an algorithm that returns ϵ -approximates ER values for all possible node pairs in the graph using $O(n^2/\epsilon)$ time. Their method is based on computing the sketches of the Laplacian matrix and its pseudoinverse. After that, [25] studied how to dynamically maintain all-pairs approximate ER values in separable graphs. In a recent work [12], based on prior work on graph sparsifiers [1], the authors presented an algorithm for the offline fully dynamic all-pairs ER problem, and further extended this idea to create data structures to maintain the approximate all-pairs ER values in fully dynamic graphs in a prediction assisted setting. [7] developed an efficient linearly convergent distributed algorithm for ER computation. The proposed algorithm is further applied to the consensus problem, which aims to compute the average of node values in a distributed manner. Since this paper focuses on handling ϵ -approximate PER queries, the problems studied in the aforementioned work are beyond the scope of this paper. Given a graph G , a *spanning tree* $T(G)$ is a subgraph of G , which includes all the nodes of G with a minimum possible number of edges [14]. Corollary 4.2 in [40] proves that $r(s, t) = \frac{|T(G')|}{|T(G)|}$, where G' be a subgraph of G obtained by identifying s and t . Besides the methods remarked in Section 2.3, Peng et al. [49] also introduced an algorithm ST for estimating ER by employing the local algorithm presented in [41] to estimate $|T(G')|$ and $|T(G)|$. We do not compare with ST since it returns $r(s, t)$ satisfying the relative approximation guarantee rather than the ϵ -approximation. As pointed out in [49], ST does not perform well in practice.

6.2 Commute Time

By definition, ER is closely pertinent to *commute time* [45]; hence we review that are relevant to estimating commute times in graphs in the sequel. Sarkar and Moore [54] proposed GRANCH, which computes the *truncated commute times* of all nodes to a target node by decomposing the input graph into overlapping neighborhoods for each node. In the subsequent work [55], they combined sampling techniques with the branch and bound pruning scheme to obtain upper and lower bounds on commute times from a node, without iterating over the entire graph. Ref. [11]

described an algorithm estimating column-wise and pair-wise commute times based on a variation of the conjugate gradient algorithm. In [17], the authors showed how to build a $O\left(\frac{n \log n}{\epsilon^2}\right)$ -size data structure in time $O(nm^{3/4} + n^{2/3}m)$, which can output a $1 + \epsilon$ multiplicative approximation to the commute time of any given pair of nodes. [34] presented a method that incrementally estimates the commute time to facilitate online applications using properties of random walks and hitting time on graphs.

6.3 Personalized PageRank

Another line of research that is germane to this work is *personalized PageRank* (PPR) [28, 32] and its variant *heat kernel PageRank* (HKPR) [16, 35]. In the past years, PPR and HKPR have been extensively studied in the literature, as surveyed in [48]. Amid them, a number of recent studies [8, 38, 39, 58, 67–71, 73, 77] propose to combine random walks with restart [23, 66] with push-operation-based deterministic graph traversal [3, 4] for improved efficiency in processing single-source or single-pair PPR/HKPR queries. At first glance, it seems that we can simply adapt and extend these techniques to ϵ -approximate PER computation. Unfortunately, contrary to PPR and HKPR, ER is inherently more sophisticated than PPR/HKPR as they differ significantly in the ways of defining random walks. In particular, the random walk model used in PPR/HKPR is *random walk with restart* [66], which would stop at each visited node on the walk with a certain probability according to geometric or Poisson distributions, whereas ER relies on simple random walks of various fixed lengths (from 1 to ∞). With a stopping probability, the random walks with restart and push-operation-based graph traversal in PPR/HKPR computation are in turn more likely to terminate after a few steps. As for ER, a linchpin to facilitate ER computation is a tight lower bound for the maximum random walk length. Consequently, it is more challenging to enable the combination of graph traversal and random walks for enhanced efficiency in ER computation.

In addition to the above similarity/dissimilarity measures, there also exist a plethora of other random walk-based measures [56, 75, 76] akin to ER, as surveyed in [40, 78].

7 CONCLUSION

This paper presents two novel probabilistic algorithms, AMC and GEER, for answering ϵ -approximate PER queries efficiently. AMC improves over the state-of-the-art approach by an optimized bound for the maximum random walk length and an adaptive sampling strategy. Particularly, AMC provides a superior time complexity while retaining the accuracy assurance. For the purpose of practical efficiency, we further develop GEER, which is built on the idea of integrating deterministic graph traversal into AMC. GEER offers significantly enhanced empirical efficiency over AMC without degrading its theoretical guarantees. Such empirical efficiency is unmatched by any existing solutions for ϵ -approximate PER computation. Our experimental results show that GEER consistently outperforms the state of the art in terms of efficiency, and is often orders of magnitude faster.

ACKNOWLEDGMENTS

This work is partially supported the National Natural Science Foundation of China (NSFC) under Grant No. U22B2060, by Guangzhou Municipal Science and Technology Bureau under Grant No. 2023A03J0667, by HKUST(GZ) under a Startup Grant, and by A*STAR Singapore under Grant A19E3b0099. The findings herein reflect the work, and are solely the responsibility, of the authors.

A PROOFS

A.1 Proof of Theorem 3.1

We first need the following lemma.

LEMMA A.1. *Given an undirected graph G , for any two nodes $u, v \in V$ and any integer $i \geq 1$, the matrix \mathbf{P} can be decomposed as*

$$p_i(u, v) = \sum_{k=1}^n \vec{\mathbf{f}}_k(u) \cdot \vec{\mathbf{f}}_k(v) \cdot \vec{\boldsymbol{\pi}}(v) \cdot \lambda_k^i, \quad (18)$$

$$\text{and } \frac{1}{\vec{\boldsymbol{\pi}}(v)} = \sum_{k=1}^n \vec{\mathbf{f}}_k^2(v), \quad (19)$$

where $1 = \lambda_1 \geq \lambda_2 \geq \dots \geq \lambda_n \geq -1$ are the eigenvalues of \mathbf{P} and $\vec{\mathbf{f}}_1, \vec{\mathbf{f}}_2, \dots, \vec{\mathbf{f}}_n$ are the corresponding eigenvectors. The eigenvector $\vec{\mathbf{f}}_1$ is taken to be $\vec{\mathbf{1}}$.

PROOF. By definition, we have $\mathbf{P}\vec{\mathbf{f}}_k = \lambda_k \vec{\mathbf{f}}_k \forall 1 \leq k \leq n$. Then, it is easy to derive that $\mathbf{P}^2 \vec{\mathbf{f}}_k = \mathbf{P} \lambda_k \vec{\mathbf{f}}_k = \lambda_k \mathbf{P} \vec{\mathbf{f}}_k = \lambda_k^2 \vec{\mathbf{f}}_k$. By repeating the above process, we obtain $\mathbf{P}^i \vec{\mathbf{f}}_k = \lambda_k^i \vec{\mathbf{f}}_k \forall i \geq 1$ and $\forall 1 \leq k \leq n$. In particular, since random walk matrix \mathbf{P} is row-stochastic, its largest eigenvalue $\lambda_1 = 1$ and the corresponding eigenvector $\vec{\mathbf{f}}_1$ can be taken to be the constant vector $\vec{\mathbf{1}}$ [27].

According to [72], $\vec{\mathbf{e}}_v = \sum_{k=1}^n \vec{\mathbf{f}}_k(v) \cdot \vec{\boldsymbol{\pi}}(v) \cdot \vec{\mathbf{f}}_k$. Hence, we get $\mathbf{P}^i(u, v) = (\mathbf{P}^i \vec{\mathbf{e}}_v)(u) = (\sum_{k=1}^n \vec{\mathbf{f}}_k(v) \cdot \vec{\boldsymbol{\pi}}(v) \cdot \mathbf{P}^i \vec{\mathbf{f}}_k)(u)$. Since $\mathbf{P}^i \vec{\mathbf{f}}_k = \lambda_k^i \vec{\mathbf{f}}_k$, substituting in the above equality gives us

$$\mathbf{P}^i(u, v) = \left(\sum_{k=1}^n \vec{\mathbf{f}}_k(v) \cdot \vec{\boldsymbol{\pi}}(v) \cdot \lambda_k^i \vec{\mathbf{f}}_k \right)(u) = \vec{\boldsymbol{\pi}}(v) \sum_{k=1}^n \vec{\mathbf{f}}_k(u) \cdot \vec{\mathbf{f}}_k(v) \cdot \lambda_k^i,$$

which is exactly Eq. (18). In addition,

$$1 = \vec{\mathbf{e}}_v \cdot \vec{\mathbf{e}}_v^\top = \sum_{k=1}^n \vec{\mathbf{f}}_k(v) \cdot \vec{\boldsymbol{\pi}}(v) \cdot \vec{\mathbf{f}}_k \vec{\mathbf{e}}_v^\top = \sum_{k=1}^n \vec{\mathbf{f}}_k^2(v) \cdot \vec{\boldsymbol{\pi}}(v),$$

which proves Eq. (19). Therefore, the lemma is proved. \square

Now, we are ready to prove Theorem 3.1.

PROOF OF THEOREM 3.1. According to Eq. (19) in Lemma A.1, the following equations hold

$$\sum_{k=1}^n \vec{\mathbf{f}}_k^2(s) = \frac{2m}{d(s)} \text{ and } \sum_{k=1}^n \vec{\mathbf{f}}_k^2(t) = \frac{2m}{d(t)}. \quad (20)$$

Note that $1 = \lambda_1 \geq \lambda_2 \geq \dots \geq \lambda_n \geq -1$. Thus, by Eq. (18), we get

$$\frac{d(t)}{2m} \sum_{k=1}^n \vec{\mathbf{f}}_k(s) \cdot \vec{\mathbf{f}}_k(t) \geq \frac{d(t)}{2m} \sum_{k=1}^n \vec{\mathbf{f}}_k(s) \cdot \vec{\mathbf{f}}_k(t) \cdot \lambda_k^2 = p_2(s, t) \geq 0. \quad (21)$$

Using Eq. (20) and Eq. (21) together with $\vec{\mathbf{f}}_1 = \vec{\mathbf{1}}$, we have that

$$\frac{1}{2m} \sum_{k=2}^n (\vec{\mathbf{f}}_k(s) - \vec{\mathbf{f}}_k(t))^2 = \frac{1}{2m} \sum_{k=1}^n (\vec{\mathbf{f}}_k(s) - \vec{\mathbf{f}}_k(t))^2 = \frac{1}{2m} \sum_{k=1}^n (\vec{\mathbf{f}}_k^2(s) + \vec{\mathbf{f}}_k^2(t) - 2\vec{\mathbf{f}}_k(s) \cdot \vec{\mathbf{f}}_k(t)) \leq \frac{1}{d(s)} + \frac{1}{d(t)}. \quad (22)$$

In addition, by Eq. (18) in Lemma A.1 and the fact $\vec{\mathbf{f}}_1 = \vec{\mathbf{1}}$,

$$\frac{p_i(s, s)}{d(s)} + \frac{p_i(t, t)}{d(t)} - \frac{2p_i(s, t)}{d(t)} = \frac{1}{2m} \sum_{k=2}^n (\vec{\mathbf{f}}_k(s) - \vec{\mathbf{f}}_k(t))^2 \cdot \lambda_k^i. \quad (23)$$

With Eq. (23) and Eq. (22), we obtain

$$\begin{aligned}
 |r(s, t) - r_\ell(s, t)| &= \left| \sum_{i=\ell+1}^{\infty} \frac{p_i(s, s)}{d(s)} + \frac{p_i(t, t)}{d(t)} - \frac{2p_i(s, t)}{d(t)} \right| = \left| \frac{1}{2m} \sum_{k=2}^n (\vec{f}_k(s) - \vec{f}_k(t))^2 \sum_{i=\ell+1}^{\infty} \lambda_k^i \right| \\
 &\leq \frac{1}{2m} \sum_{k=2}^n (\vec{f}_k(s) - \vec{f}_k(t))^2 \sum_{i=\ell+1}^{\infty} \lambda^i = \frac{\lambda^{\ell+1}}{1-\lambda} \cdot \frac{1}{2m} \sum_{k=2}^n (\vec{f}_k(s) - \vec{f}_k(t))^2 \\
 &\leq \frac{\lambda^{\ell+1}}{1-\lambda} \cdot \left(\frac{1}{d(s)} + \frac{1}{d(t)} \right).
 \end{aligned}$$

Plugging Eq. (6) into the above inequality yields $|r(s, t) - r_\ell(s, t)| \leq \frac{\epsilon}{2}$, which proves the theorem. \square

A.2 Proof of Lemma 3.3

PROOF. Consider a length- ℓ_f random walk W from u which contains ℓ_f visited nodes $\{w_1, w_2, \dots, w_{\ell_f}\}$. Note for any $1 \leq i \leq \ell_f$, w_i and w_{i+1} are two adjacent nodes. This implies that for any node $v \in V$, it appears at most $\left\lceil \frac{\ell_f}{2} \right\rceil$ times. Let W_1 contain $\left\lceil \frac{\ell_f}{2} \right\rceil$ nodes of W with the largest values with respect to $\vec{x}(\cdot)$ and W_2 contain the remaining $\left\lfloor \frac{\ell_f}{2} \right\rfloor$ nodes. Hence,

$$\sum_{w \in W} \vec{x}(w) = \sum_{w \in W_1} \vec{x}(w) + \sum_{w \in W_2} \vec{x}(w) \leq \left\lceil \frac{\ell_f}{2} \right\rceil \cdot \max_1(\vec{x}) + \left\lfloor \frac{\ell_f}{2} \right\rfloor \cdot \max_2(\vec{x}).$$

Note that $\sum_{w \in W} \vec{x}(w) \geq \ell_f \cdot \min(\vec{x})$ and the lemma follows. \square

A.3 Proof of Theorem 3.4

PROOF. Letting $Z'_k := Z_k + \frac{\psi}{2}$, we immediately have $0 \leq Z'_k \leq \psi$. Then, the empirical mean $Z' = Z + \frac{\psi}{2}$ and empirical variance remains the same $\hat{\sigma}^2$. Let T be the stopping time. If Algorithm 1 stops at the i -th iteration such that $i < \tau$, we know $f(\eta, \hat{\sigma}^2, \psi, \delta/\tau) \leq \frac{\epsilon}{2}$. Thus, given $i < \tau$, using the Bernstein inequality (Lemma 3.2), we obtain

$$\begin{aligned}
 \mathbb{P}[|Z - \mathbb{E}[Z]| > \frac{\epsilon}{2} \wedge T = i] &\leq \mathbb{P}[|Z - \mathbb{E}[Z]| \geq f(\eta, \hat{\sigma}^2, \psi, \frac{\delta}{\tau}) \wedge T = i] \\
 &= \mathbb{P}[|Z' - \mathbb{E}[Z']| \geq f(\eta, \hat{\sigma}^2, \psi, \frac{\delta}{\tau}) \wedge T = i] \leq \frac{\delta}{\tau}.
 \end{aligned}$$

In addition, consider that $T = \tau$. According to the Hoeffding's inequality (Lemma 2.3), we have

$$\mathbb{P}[|Z - \mathbb{E}[Z]| > \frac{\epsilon}{2} \wedge T = \tau] \leq 2 \exp\left(-\frac{\eta \epsilon^2}{2\psi^2}\right) \leq 2 \exp\left(-\frac{\eta^* \epsilon^2}{2\psi^2}\right) = \frac{\delta}{\tau}.$$

Putting it together yields $\mathbb{P}[|Z - \mathbb{E}[Z]| > \frac{\epsilon}{2}] \leq (\tau - 1) \cdot \frac{\delta}{\tau} + \frac{\delta}{\tau} = \delta$, which immediately concludes that $|r_f(s, t) - q(s, t)| \leq \frac{\epsilon}{2}$ holds with a probability of at least $1 - \delta$, since $r_f(s, t) = Z$ and $q(s, t) = \mathbb{E}[Z]$.

Moreover, when setting $\ell_f = \ell$ as in Eq. (6), $\vec{s} = \vec{e}_s$ and $\vec{t} = \vec{e}_t$, by Theorem 3.1, we know that $|r(s, t) - r_\ell(s, t)| \leq \frac{\epsilon}{2}$. Meanwhile,

$$q(s, t) = \sum_{i=1}^{\ell} \left(\frac{p_i(s, s)}{d(s)} + \frac{p_i(t, t)}{d(t)} - \frac{p_i(s, t)}{d(t)} - \frac{p_i(t, s)}{d(s)} \right) = r_\ell(s, t) - \mathbb{1}_{s \neq t} \cdot \left(\frac{1}{d(s)} + \frac{1}{d(t)} \right),$$

Therefore, with a probability of at least $1 - \delta$, we have

$$\begin{aligned}
 \left| r_f(s, t) + \mathbb{1}_{s \neq t} \cdot \left(\frac{1}{d(s)} + \frac{1}{d(t)} \right) - r(s, t) \right| &\leq \left| r_f(s, t) + \mathbb{1}_{s \neq t} \cdot \left(\frac{1}{d(s)} + \frac{1}{d(t)} \right) - r_\ell(s, t) \right| + |r_\ell(s, t) - r(s, t)| \\
 &\leq \frac{\epsilon}{2} + \frac{\epsilon}{2} = \epsilon.
 \end{aligned}$$

This completes the proof. \square

REFERENCES

- [1] Ittai Abraham, David Durfee, Ioannis Koutis, Sebastian Krininger, and Richard Peng. 2016. On fully dynamic graph sparsifiers. In *IEEE Annual Symposium on Foundations of Computer Science (FOCS)*. 335–344.
- [2] Vedat Levi Alev, Nima Anari, Lap Chi Lau, and Shayan Oveis Gharan. 2018. Graph Clustering using Effective Resistance. In *Innovations in Theoretical Computer Science (ITCS)*, Vol. 94. 41.
- [3] Reid Andersen, Christian Borgs, Jennifer Chayes, John Hopcraft, Vahab S Mirrokni, and Shang-Hua Teng. 2007. Local computation of PageRank contributions. In *WAM*. 150–165.
- [4] Reid Andersen, Fan Chung, and Kevin Lang. 2006. Local graph partitioning using pagerank vectors. In *IEEE Annual Symposium on Foundations of Computer Science (FOCS)*. 475–486.
- [5] Alexandr Andoni, Robert Krauthgamer, and Yosef Poghrow. 2018. On Solving Linear Systems in Sublinear Time. In *Innovations in Theoretical Computer Science (ITCS)*.
- [6] Jean-Yves Audibert, Rémi Munos, and Csaba Szepesvári. 2007. Tuning bandit algorithms in stochastic environments. In *ALT*. 150–165.
- [7] Necdet Serhat Aybat and Mert Gürbüzbalaban. 2017. Decentralized computation of effective resistances and acceleration of consensus algorithms. In *GlobalSIP*. 538–542.
- [8] Siddhartha Banerjee and Peter Lofgren. 2015. Fast Bidirectional Probability Estimation in Markov Models. *Advances in Neural Information Processing Systems (NeurIPS)* (2015), 1423–1431.
- [9] Régis Behmo, Nikos Paragios, and Véronique Prinet. 2008. Graph commute times for image representation. In *IEEE Conference on Computer Vision and Pattern Recognition (CVPR)*. 1–8.
- [10] András A Benczúr and David R Karger. 1996. Approximating s - t minimum cuts in $\tilde{O}(n^2)$ time. In *Proceedings of the Annual ACM Symposium on Theory of computing (STOC)*. 47–55.
- [11] Francesco Bonchi, Pooya Esfandiari, David F Gleich, Chen Greif, and Laks VS Lakshmanan. 2012. Fast matrix computations for pairwise and columnwise commute times and Katz scores. *Internet Mathematics* (2012), 73–112.
- [12] Felix Broberg. 2020. Prediction Assisted Fully Dynamic All-Pairs Effective Resistance.
- [13] Ashok K Chandra, Prabhakar Raghavan, Walter L Ruzzo, Roman Smolensky, and Prason Tiwari. 1996. The electrical resistance of a graph captures its commute and cover times. *computational complexity* (1996), 312–340.
- [14] David Cheriton and Robert Endre Tarjan. 1976. Finding minimum spanning trees. *SIAM J. Comput.* (1976), 724–742.
- [15] Paul Christiano, Jonathan A Kelner, Aleksander Madry, Daniel A Spielman, and Shang-Hua Teng. 2011. Electrical flows, laplacian systems, and faster approximation of maximum flow in undirected graphs. In *Proceedings of the Annual ACM Symposium on Theory of computing (STOC)*. 273–282.
- [16] Fan Chung. 2007. The heat kernel as the pagerank of a graph. *Proceedings of the National Academy of Sciences (PNAS)* 104, 50 (2007), 19735–19740.
- [17] Michael B Cohen, Jonathan Kelner, John Peebles, Richard Peng, Aaron Sidford, and Adrian Vladu. 2016. Faster algorithms for computing the stationary distribution, simulating random walks, and more. In *IEEE Annual Symposium on Foundations of Computer Science (FOCS)*. 583–592.
- [18] Michael B Cohen, Rasmus Kyng, Gary L Miller, Jakub W Pachocki, Richard Peng, Anup B Rao, and Shen Chen Xu. 2014. Solving SDD linear systems in nearly $m \log^{1/2} n$ time. In *Proceedings of the Annual ACM Symposium on Theory of computing (STOC)*. 343–352.
- [19] Thomas H Cormen, Charles E Leiserson, Ronald L Rivest, and Clifford Stein. 2009. *Introduction to algorithms*. MIT press.
- [20] Atish Das Sarma, Danupon Nanongkai, Gopal Pandurangan, and Prasad Tetali. 2013. Distributed random walks. *JACM* 60, 1 (2013), 1–31.
- [21] James W Demmel. 1997. *Applied numerical linear algebra*. SIAM.
- [22] Florian Dörfler and Francesco Bullo. 2010. Spectral analysis of synchronization in a lossless structure-preserving power network model. In *IEEE International Conference on Smart Grid Communications*. 179–184.
- [23] Dániel Fogaras, Balázs Rácz, Károly Csalogány, and Tamás Sarlós. 2005. Towards scaling fully personalized pagerank: Algorithms, lower bounds, and experiments. *Internet Mathematics* (2005), 333–358.
- [24] Francois Fouss, Alain Pirotte, Jean-Michel Renders, and Marco Saerens. 2007. Random-walk computation of similarities between nodes of a graph with application to collaborative recommendation. *IEEE Transactions on Knowledge and Data Engineering (TKDE)* 19, 3 (2007), 355–369.
- [25] Gramoz Goranci, Monika Henzinger, and Pan Peng. 2018. Dynamic Effective Resistances and Approximate Schur Complement on Separable Graphs. In *ESA*.
- [26] Linqi Guo, Chen Liang, and Steven H Low. 2017. Monotonicity properties and spectral characterization of power redistribution in cascading failures. In *Allerton*. 918–925.
- [27] Taher Haveliwala and Sepandar Kamvar. 2003. *The second eigenvalue of the Google matrix*. Technical Report. Stanford.
- [28] Taher H Haveliwala. 2002. Topic-sensitive PageRank. In *The Web Conference (WWW)*. 517–526.

- [29] Takanori Hayashi, Takuya Akiba, and Yuichi Yoshida. 2016. Efficient Algorithms for Spanning Tree Centrality. In *Proceedings of the International Joint Conference on Artificial Intelligence (IJCAI)*, Vol. 16. 3733–3739.
- [30] Wassily Hoeffding. 1963. Probability Inequalities for Sums of Bounded Random Variables. *J. Amer. Statist. Assoc.* 58, 301 (1963), 13–30.
- [31] Arun Jambulapati and Aaron Sidford. 2018. Efficient $\tilde{O}(n/\epsilon)$ Spectral Sketches for the Laplacian and its Pseudoinverse. In *Proceedings of the Annual ACM-SIAM Symposium on Discrete Algorithms (SODA)*. 2487–2503.
- [32] Glen Jeh and Jennifer Widom. 2003. Scaling personalized web search. In *The Web Conference (WWW)*. 271–279.
- [33] Jonathan A Kelner, Yin Tat Lee, Lorenzo Orecchia, and Aaron Sidford. 2014. An almost-linear-time algorithm for approximate max flow in undirected graphs, and its multicommodity generalizations. In *Proceedings of the Annual ACM-SIAM Symposium on Discrete Algorithms (SODA)*. 217–226.
- [34] Nguyen Lu Dang Khoa, Yang Wang, and Sanjay Chawla. 2019. Incremental commute time and its online applications. *Pattern Recognition* (2019), 101–112.
- [35] Kyle Kloster and David F Gleich. 2014. Heat kernel based community detection. In *Proceedings of the ACM International Conference on Knowledge Discovery and Data Mining (SIGKDD)*. 1386–1395.
- [36] Jérôme Kunegis and Stephan Schmidt. 2007. Collaborative filtering using electrical resistance network models. In *International Conference on Data Mining (ICDM)*. 269–282.
- [37] Richard B Lehoucq, Danny C Sorensen, and Chao Yang. 1998. *ARPACK users' guide: solution of large-scale eigenvalue problems with implicitly restarted Arnoldi methods*. SIAM.
- [38] Peter Lofgren, Siddhartha Banerjee, and Ashish Goel. 2015. Bidirectional PageRank Estimation: From Average-Case to Worst-Case. In *International Workshop on Algorithms and Models for the Web-Graph (WAW)*. 164–176.
- [39] Peter Lofgren, Siddhartha Banerjee, and Ashish Goel. 2016. Personalized pagerank estimation and search: A bidirectional approach. In *Proceedings of the ACM International Conference on Web Search and Data Mining (WSDM)*. 163–172.
- [40] László Lovász. 1993. Random walks on graphs: a survey. *Combinatorics, Paul erdos is eighty* 2, 4 (1993), 1–46.
- [41] Russell Lyons and Shayan Oveis Gharan. 2018. Sharp bounds on random walk eigenvalues via spectral embedding. *International Mathematics Research Notices* 2018, 24 (2018), 7555–7605.
- [42] Charalampos Mavroforakis, Richard Garcia-Lebron, Ioannis Koutis, and Evimaria Terzi. 2015. Spanning edge centrality: Large-scale computation and applications. In *The Web Conference (WWW)*. 732–742.
- [43] Julian J McAuley and Jure Leskovec. 2012. Learning to discover social circles in ego networks.. In *Advances in Neural Information Processing Systems (NeurIPS)*. 548–56.
- [44] Volodymyr Mnih, Csaba Szepesvári, and Jean-Yves Audibert. 2008. Empirical bernstein stopping. In *Proceedings of the International Conference on Machine learning (ICML)*. 672–679.
- [45] Rajeev Motwani and Prabhakar Raghavan. 1995. *Randomized algorithms*. Cambridge University Press.
- [46] C St JA Nash-Williams. 1959. Random walk and electric currents in networks. In *Math. Proc. Camb. Philos. Soc.* Cambridge University Press, 181–194.
- [47] James William Nilsson. 2008. *Electric circuits*. Pearson Education India.
- [48] Sungchan Park, Wonseok Lee, Byeongseo Choe, and Sang-Goo Lee. 2019. A survey on personalized PageRank computation algorithms. *IEEE Access* (2019), 163049–163062.
- [49] Pan Peng, Daniel Lopatta, Yuichi Yoshida, and Gramoz Goranci. 2021. Local Algorithms for Estimating Effective Resistance. In *Proceedings of the ACM International Conference on Knowledge Discovery and Data Mining (SIGKDD)*. 1329–1338.
- [50] Huaijun Qiu and Edwin R Hancock. 2005. Image Segmentation using Commute Times.. In *BMVC*. 929–938.
- [51] Huaijun Qiu and Edwin R Hancock. 2007. Clustering and embedding using commute times. *IEEE Transactions on Pattern Analysis and Machine Intelligence (TPAMI)* 29, 11 (2007), 1873–1890.
- [52] Jiezhong Qiu, Laxman Dhulipala, Jie Tang, Richard Peng, and Chi Wang. 2021. Lightne: A lightweight graph processing system for network embedding. In *Proceedings of the International Conference on Management of Data (SIGMOD)*. 2281–2289.
- [53] Ran Raz. 2002. On the complexity of matrix product. In *Proceedings of the Annual ACM Symposium on Theory of computing (STOC)*. 144–151.
- [54] Purnamrita Sarkar and Andrew W Moore. 2007. A tractable approach to finding closest truncated-commute-time neighbors in large graphs. In *Proceedings of the Conference on Uncertainty in Artificial Intelligence (UAI)*. 335–343.
- [55] Purnamrita Sarkar, Andrew W Moore, and Amit Prakash. 2008. Fast incremental proximity search in large graphs. In *Proceedings of the International Conference on Machine learning (ICML)*. 896–903.
- [56] Jieming Shi, Tianyuan Jin, Renchi Yang, Xiaokui Xiao, and Yin Yang. 2020. Realtime index-free single source SimRank processing on web-scale graphs. *Proceedings of the VLDB Endowment* 13, 7 (2020), 966–980.
- [57] Jieming Shi, Nikos Mamoulis, Dingming Wu, and David W Cheung. 2014. Density-based place clustering in geo-social networks. In *Proceedings of the International Conference on Management of Data (SIGMOD)*. 99–110.

- [58] Jieming Shi, Renchi Yang, Tianyuan Jin, Xiaokui Xiao, and Yin Yang. 2019. Realtime top-k personalized pagerank over large graphs on gpus. *Proceedings of the VLDB Endowment (PVLDB)* 13, 1 (2019), 15–28.
- [59] Saleh Soltan, Dorian Mazauric, and Gil Zussman. 2015. Analysis of failures in power grids. *IEEE Transactions on Control of Network Systems* 4, 2 (2015), 288–300.
- [60] Yue Song, David J Hill, and Tao Liu. 2017. Network-based analysis of small-disturbance angle stability of power systems. *IEEE Transactions on Control of Network Systems* 5, 3 (2017), 901–912.
- [61] Yue Song, David J Hill, and Tao Liu. 2019. On extension of effective resistance with application to graph laplacian definiteness and power network stability. *IEEE Transactions on Circuits and Systems I: Regular Papers* 66, 11 (2019), 4415–4428.
- [62] Daniel A Spielman and Nikhil Srivastava. 2008. Graph sparsification by effective resistances. *Proceedings of the Annual ACM Symposium on Theory of computing (STOC)*, 563–568.
- [63] Daniel A Spielman and Shang-Hua Teng. 2004. Nearly-linear time algorithms for graph partitioning, graph sparsification, and solving linear systems. In *Proceedings of the Annual ACM Symposium on Theory of computing (STOC)*. 81–90.
- [64] Kumar Sricharan and Kamalika Das. 2014. Localizing anomalous changes in time-evolving graphs. In *Proceedings of the International Conference on Management of Data (SIGMOD)*. 1347–1358.
- [65] Prasad Tetali. 1991. Random walks and the effective resistance of networks. *Journal of Theoretical Probability* 4, 1 (1991), 101–109.
- [66] Hanghang Tong, Christos Faloutsos, and Jia-Yu Pan. 2006. Fast random walk with restart and its applications. In *International Conference on Data Mining (ICDM)*. 613–622.
- [67] Hanzhi Wang, Mingguo He, Zhewei Wei, Sibow Wang, Ye Yuan, Xiaoyong Du, and Ji-Rong Wen. 2021. Approximate Graph Propagation. In *Proceedings of the ACM International Conference on Knowledge Discovery and Data Mining (SIGKDD)*. 1686–1696.
- [68] Sibow Wang, Youze Tang, Xiaokui Xiao, Yin Yang, and Zengxiang Li. 2016. HubPPR: effective indexing for approximate personalized pagerank. *Proceedings of the VLDB Endowment (PVLDB)* 10, 3 (2016), 205–216.
- [69] Sibow Wang, Renchi Yang, Runhui Wang, Xiaokui Xiao, Zhewei Wei, Wenqing Lin, Yin Yang, and Nan Tang. 2019. Efficient algorithms for approximate single-source personalized pagerank queries. *ACM Transactions on Database Systems (TODS)* 44, 4 (2019), 1–37.
- [70] Sibow Wang, Renchi Yang, Xiaokui Xiao, Zhewei Wei, and Yin Yang. 2017. FORA: simple and effective approximate single-source personalized pagerank. In *Proceedings of the ACM International Conference on Knowledge Discovery and Data Mining (SIGKDD)*. 505–514.
- [71] Zhewei Wei, Xiaodong He, Xiaokui Xiao, Sibow Wang, Shuo Shang, and Ji-Rong Wen. 2018. Topppr: top-k personalized pagerank queries with precision guarantees on large graphs. In *Proceedings of the International Conference on Management of Data (SIGMOD)*. 441–456.
- [72] EL Wilmer, David A Levin, and Yuval Peres. 2009. Markov chains and mixing times. *American Mathematical Soc., Providence* (2009).
- [73] Hao Wu, Junhao Gan, Zhewei Wei, and Rui Zhang. 2021. Unifying the Global and Local Approaches: An Efficient Power Iteration with Forward Push. In *Proceedings of the International Conference on Management of Data (SIGMOD)*. 1996–2008.
- [74] Jaewon Yang and Jure Leskovec. 2012. Defining and Evaluating Network Communities Based on Ground-Truth. In *International Conference on Data Mining (ICDM)*. 745–754.
- [75] Renchi Yang. 2022. Efficient and Effective Similarity Search over Bipartite Graphs. In *Proceedings of the ACM Web Conference 2022*. 308–318.
- [76] Renchi Yang and Xiaokui Xiao. 2021. Fast Approximate All Pairwise CoSimRanks via Random Projection. In *International Conference on Web Information Systems Engineering*. 438–452.
- [77] Renchi Yang, Xiaokui Xiao, Zhewei Wei, Sourav S Bhowmick, Jun Zhao, and Rong-Hua Li. 2019. Efficient estimation of heat kernel pagerank for local clustering. In *Proceedings of the International Conference on Management of Data (SIGMOD)*. 1339–1356.
- [78] Luh Yen, Marco Saerens, Amin Mantrach, and Masashi Shimbo. 2008. A family of dissimilarity measures between nodes generalizing both the shortest-path and the commute-time distances. In *Proceedings of the ACM International Conference on Knowledge Discovery and Data Mining (SIGKDD)*. 785–793.
- [79] Luh Yen, Denis Vanvyve, Fabien Wouters, François Fous, Michel Verleysen, Marco Saerens, et al. 2005. Clustering using a random walk based distance measure. In *ESANN*. 317–324.
- [80] Hongzhi Yin, Bin Cui, Jing Li, Junjie Yao, and Chen Chen. 2012. Challenging the long tail recommendation. *Proceedings of the VLDB Endowment (PVLDB)* 5, 9 (2012), 896–907.
- [81] Xiaohan Zhao, Adelbert Chang, Atish Das Sarma, Haitao Zheng, and Ben Y Zhao. 2013. On the embeddability of random walk distances. *Proceedings of the VLDB Endowment (PVLDB)* 6, 14 (2013), 1690–1701.

Received April 2022; revised July 2022; accepted August 2022